FRA-76-27
REPORT NO. FRA/ORD-77/17

THE CAUSE OF THERMAL FATIGUE CRACKING IN METROLINER WHEELS

G.F. Carpenter

United States Steel Corporation
Research Laboratory
Monroeville PA 15146

MARCH 1977

FINAL REPORT

Prepared for

U.S. DEPARTMENT OF TRANSPORTATION
FEDERAL RAILROAD ADMINISTRATION
Research and Development
Washington DC 20590

NOTICE

This document is disseminated under the sponsorship of the Department of Transportation in the interest of information exchange. The United States Government assumes no liability for its contents or use thereof.

NOTICE

The United States Government does not endorse products or manufacturers. Trade or manufacturers' names appear herein solely because they are considered essential to the object of this report.

Technical Report Documentation Page

1. Report No.	2. Government Accession No.	3. Recipient's Catalog No.
FRA/ORD-77/17		

4. Title and Subtitle	5. Report Date
THE CAUSE OF THERMAL FATIGUE CRACKING IN METROLINER WHEELS	March 1977
	6. Performing Organization Code
7. Author(s)	8. Performing Organization Report No.
G.F. Carpenter	DOT-TSC-FRA-76-27 10-D-033(018-2)
9. Performing Organization Name and Address	10. Work Unit No. (TRAIS)
United States Steel Corporation* Research Laboratory Monroeville PA 15146	RR628/R7323
	11. Contract or Grant No.
	DOT-TSC-712
	13. Type of Report and Period Covered
12. Sponsoring Agency Name and Address	Final Report May 1974-August 1975
U.S. Department of Transportation Federal Railroad Administration Research and Development Washington DC 20590	14. Sponsoring Agency Code

15. Supplementary Notes

*Under contract to: U.S. Department of Transportation
Transportation Systems Center
Kendall Square
Cambridge MA 02142

16. Abstract

One new wheel and two used wheels (one with a thermal crack in the tread) were examined for mechanical properties, macrostructure, microstructure, and residual stresses. Similar examinations were conducted on three new wheels which were first subjected to various braking cycles designed to define the conditions that produce cracking. The braking tests were conducted on the laboratory dynamometer.

The results of this study indicated that the wheel that had developed a thermal crack in service had been intermittently and severely heated around the tread surface and that such heating had altered the microstructure, produced residual tensile stresses and permitted the crack to initiate.

The results further showed that neither altered microstructures nor cracking could be produced by many emergency brakings or speed-reduction brakings with normal brake shoes and forces.

17. Key Words	18. Distribution Statement
Metroliner Wheels Residual Thermal Stresses Thermal Cracking Macrostructure Microstructure	DOCUMENT IS AVAILABLE TO THE U.S. PUBLIC THROUGH THE NATIONAL TECHNICAL INFORMATION SERVICE, SPRINGFIELD, VIRGINIA 22161

19. Security Classif. (of this report)	20. Security Classif. (of this page)	21. No. of Pages	22. Price
Unclassified	Unclassified	92	

Form DOT F 1700.7 (8-72) Reproduction of completed page authorized

PREFACE

The research and testing studies documented in this report were carried out as part of the component failure prevention program conducted by United States Steel Corporation Research Laboratory, Monroeville PA, under contract DOT-TSC-712 for the Transportation Systems Center, U.S. Department of Transportation, Cambridge MA, under the auspices of the Federal Railroad Administion, U.S. Department of Transportation.

The work at United States Steel Corporation was subcontracted to USS Engineers and Consultants, Inc., and was carried out under the general supervision of G. P. Carpenter with interest and support by the late J. W. Lyons of DOT/TSC.

METRIC CONVERSION FACTORS

Approximate Conversions to Metric Measures

Symbol	When You Know	Multiply by	To Find	Symbol
		LENGTH		
in	inches	2.5	centimeters	cm
ft	feet	30	centimeters	cm
yd	yards	0.9	meters	m
mi	miles	1.6	kilometers	km
		AREA		
in^2	square inches	6.5	square centimeters	cm^2
ft^2	square feet	0.09	square meters	m^2
yd^2	square yards	0.8	square meters	m^2
mi^2	square miles	2.6	square kilometers	km^2
	acres	0.4	hectares	ha
		MASS (weight)		
oz	ounces	28	grams	g
lb	pounds	0.45	kilograms	kg
	short tons (2000 lb)	0.9	tonnes	t
		VOLUME		
tsp	teaspoons	5	milliliters	ml
Tbsp	tablespoons	15	milliliters	ml
fl oz	fluid ounces	30	milliliters	ml
c	cups	0.24	liters	l
pt	pints	0.47	liters	l
qt	quarts	0.95	liters	l
gal	gallons	3.8	liters	l
ft^3	cubic feet	0.03	cubic meters	m^3
yd^3	cubic yards	0.76	cubic meters	m^3
		TEMPERATURE (exact)		
°F	Fahrenheit temperature	5/9 (after subtracting 32)	Celsius temperature	°C

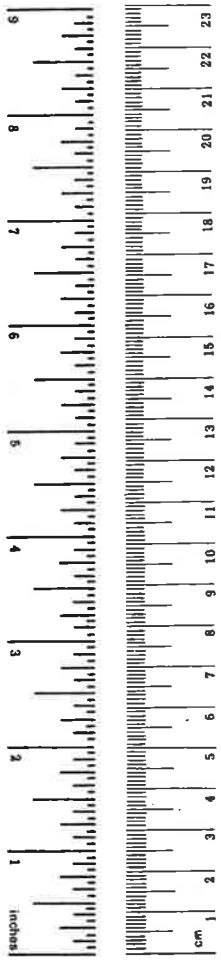

Approximate Conversions from Metric Measures

Symbol	When You Know	Multiply by	To Find	Symbol
		LENGTH		
mm	millimeters	0.04	inches	in
cm	centimeters	0.4	inches	in
m	meters	3.3	feet	ft
m	meters	1.1	yards	yd
km	kilometers	0.6	miles	mi
		AREA		
cm^2	square centimeters	0.16	square inches	in^2
m^2	square meters	1.2	square yards	yd^2
km^2	square kilometers	0.4	square miles	mi^2
ha	hectares (10,000 m^2)	2.5	acres	
		MASS (weight)		
g	grams	0.035	ounces	oz
kg	kilograms	2.2	pounds	lb
t	tonnes (1000 kg)	1.1	short tons	
		VOLUME		
ml	milliliters	0.03	fluid ounces	fl oz
l	liters	2.1	pints	pt
l	liters	1.06	quarts	qt
l	liters	0.26	gallons	gal
m^3	cubic meters	35	cubic feet	ft^3
m^3	cubic meters	1.3	cubic yards	yd^3
		TEMPERATURE (exact)		
°C	Celsius temperature	9/5 (then add 32)	Fahrenheit temperature	°F

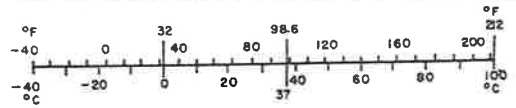

TABLE OF CONTENTS

TABLE OF CONTENTS (CONTINUED)

LIST OF ILLUSTRATIONS

LIST OF ILLUSTRATIONS (CONTINUED)

LIST OF ILLUSTRATIONS (CONTINUED)

LIST OF TABLES

1. INTRODUCTION

The Metroliner high-speed passenger train, operated by the Penn Central Railroad for Amtrak between Washington, D.C., and New York City, is equipped with dynamic brakes and on-tread friction brakes actuated by independent brake cylinders on each wheel. In normal operation, the dynamic brakes are used to decelerate from high speeds, and both the dynamic and the tread brakes are used at intermediate speeds. At low speeds, dynamic braking is ineffective; therefore, only tread braking is used. The two braking modes are blended automatically to provide optimum passenger comfort.

In the past, the dynamic-braking system on Metroliner cars has been reported to fail often, making it necessary to use the tread brakes from speeds as high as 120 mph (193 km/hr); such on-tread braking would be used until the dynamic-braking system was repaired. The treads and flanges of Metroliner wheels have been said to develop thermal cracks, even though the wheels have been made from steel with a carbon content of less than 0.47 percent, the most thermal-crack-resistant wheel-steel composition commercially available. Metroliner wheels are inspected frequently; those containing thermal cracks are immediately removed from service, since it is believed that under certain operating conditions such cracks may initiate hazardous sudden wheel failures.

Because of the Metroliner wheel problem and the need for experimental data of general applicability, the Department of Transportation (DOT) contracted with USS Engineers and Consultants, Inc., to determine the effect of various braking conditions on the tendency to develop thermal-fatigue cracks in Metroliner wheels. The original program of study comprised the evaluation of residual stresses, mechanical properties, and metallurgical characteristics of four new and two used wheels after the wheels were subjected to various numbers of emergency stops on the wheel-test machine at U.S. Steel's Research Laboratory. Unexpectedly, the first new wheel, when tested on the wheel-test machine (Appendix A), failed to develop any thermal cracks after being subjected to 300 emergency

stops from 130 mph (209 km/hr), with an inertial load of 24,100 pounds (107.2 kN) and a brakeshoe force of 7,000 pounds (31.14 kN). This is more than three times the number of stops that had been received by the used wheels in service, one of which contained a thermal crack in the tread.

Therefore, by agreement with DOT, the program of study was revised as shown in Table 1. The revised program included determination of residual stresses (1) in the wheel already subjected to 300 emergency stops, (2) in a wheel subjected to speed-reduction tests, and (3) in a wheel subjected to abnormal braking consisting of braking, stop braking with normal brakeshoes, and stop braking with simulated "wornout" brakeshoes. The foregoing represent conditions reportedly encountedly encounted in service.

This final report summarizes the results of the studies conducted on the four new and the two used Metroliner wheels in accordance with the program as agreed upon with DOT.

TABLE 1. REVISED PROGRAM FOR EVALUATION OF METROLINER WHEELS

Wheel No.	Manufacturer's Serial No.	Condition	Dynamometer Tests	Metallurgical Studies
1	1-72-S-2476A	New	300 Emergency stops from 130 mph	*
2	1-72-S-2474A	New	2424 Speed reductions (100 to 50 mph)	*
3	1-72-S-2472A	New	Four 30-minute drag-brake periods at 45 mph plus 110 emergency stops from 130 mph, 10 of which were made with a "worn-out" brake shoe	*
4	1-72-S-2466A	New	None	*
5	1-71-S-10191A	Used, with one crack in tread	None	*
6	1-71-S-10190A	Used, with no cracks	None	*

* All wheels were examined for chemical composition, mechanical properties, macrostructure, and microstructure.

Conversion Factor

1 mph = 1.61 km/hr

2. MATERIALS AND EXPERIMENTAL WORK

2.1 MATERIALS

The six rim-treated Section B-36, Class A (0.4% carbon) wrought-steel wheels studied were produced by the Standard Steel Division of Titanium Metals Corporation of America. The chemical composition of the wheels is shown in Table 2, along with the specified range for AAR Specification M-107, Class A wheels. The plate surfaces of the wheels had been contour-machined and shot-peened.

The new wheels (Nos. 1 through 4) were produced in January 1972 and were selected from stock at the Penn Central shops in Wilmington, Delaware. Both used wheels (Nos. 5 and 6) were produced in January 1971 and had been in service on Metroliner axle No. W80829, car No. 864, from November 7, 1971, to June 23, 1972. During this period, the wheels were used for a total of about 100,000 miles (160,000 km), but the dynamic-braking system was inoperative for about 1610 miles (2590 km). It was estimated that the wheels had been subjected to 85 station stops from normal operating speeds and to numerous speed-reduction brake applications without the assistance of the dynamic brakes. Wheel No. 5 exhibited a fatigue-type thermal crack, which measured about 1-1/4 inches (32 mm) long on the tread, but wheel No. 6 had no apparent cracks. The other six wheels on the car were reported to be crack-free, as determined by magnetic-particle tests conducted by Penn Central.

Wheels No. 1, 2, and 3 were subjected to various braking conditions on the wheel-test machine, to metallurgical studies, and to residual-stress studies. Wheels No. 4, 5, and 6 were subjected only to metallurgical and residual-stress studies.

2.2 METALLURGICAL STUDIES

As indicated in Figure 1, the following metallurgical studies were conducted on the wheels:

TABLE 2. CHEMICAL COMPOSITION OF METROLINER WHEELS (RESEARCH LABORATORY CHECK ANALYSIS)

Wheel No.	Manufacturer's Number	Chemical Composition, percent										
		C	Mn	P	S	Si	Cu	Ni	Cr	Mo	Ti	Total Al
1	1-72-S-2476A	0.42	0.80	0.017	0.026	0.31	0.083	0.061	0.051	0.018	0.014	0.005
2	1-72-S-2474A	0.42	0.77	0.022	0.036	0.29	0.136	0.075	0.083	0.017	0.013	0.007
3	1-72-S-2472A	0.42	0.76	0.024	0.030	0.30	0.121	0.071	0.075	0.020	0 013	0 006
4	1-72-S-2466A	0.43	0.80	0.022	0.035	0.32	0.127	0.076	0.077	0.022	0.014	0.004
5	1-71-S-10191A	0.43	0.79	0.022	0.041	0.33	0.179	0.068	0.154	0.033	0.016	0.013
6	1-71-S-10190A	0.42	0.76	0.014	0.032	0.31	0.080	0.041	0.057	0.017	0.012	0.004
	AAR Specification M-107-71 for Class A Wheels, Wrought Carbon Steel	0.57* max	0.60 / 0.85	0.05 max	0.05 max	0.15 min	+	+	+	+	+	+

*The carbon content of Class A wheels normally ranges from 0.47 to 0.57 percent.
+ Not specified.

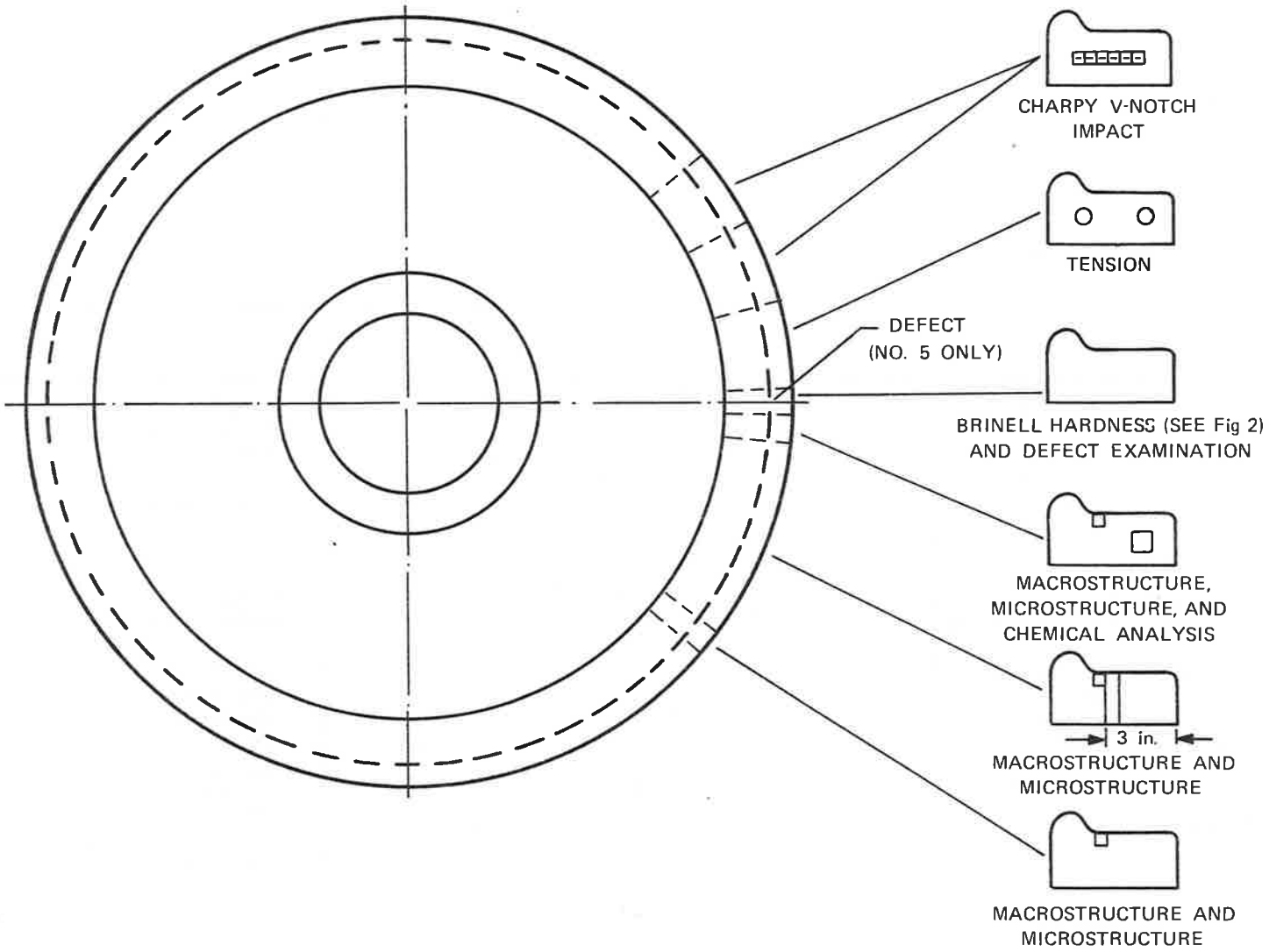

FIGURE 1. LOCATION OF METALLURGICAL SPECIMENS

1. The chemical composition of each rim was determined for a specimen from the midwidth-midthickness position.

2. The tensile properties of each rim were determined by testing 0.252-inch-diameter (6.4 mm) circumferentially oriented (chordal) tension-test specimens removed from the midthickness-quarterwidth position.

3. The impact properties of each rim were determined by testing circumferentially-oriented (chordal) Charpy V-notch specimens removed from the midthickness-quarterwidth position.

4. Brinell hardness tests were conducted on a radial-axial section of the rim of each wheel at the locations shown in Figure 2.

5. The fatigue-type thermal crack in wheel No. 5 was visually examined after the rim was fractured (in the Laboratory) through the existing crack. In addition, the tread surface of each wheel was examined for surface defects by the fluorescent-magnetic-particle method.

6. Several radial and radial-tangential sections of each rim were etched in nital, and their macrostructures were examined.

7. Selected specimens from the rim were also etched in picral reagent, and their microstructures were examined.

8. The diamond-pyramid hardness of selected metallographic specimens were determined with a Vickers microhardness tester with a load of 2.5 kg.

2.3 DYNAMOMETER TESTS

2.3.1 Emergency-Stop-Braking Conditions for Wheel No. 1

The conditions for simulated emergency-stop braking of wheel No. 1 are shown in Table 3. In Metroliner service, the inertial wheel load (gross car weight divided by number of wheels) is 23,100 pounds (102.75 kN). Therefore, the inertial wheel load for these tests on U.S. Steel's wheel-test dynamometer was set at 24,100

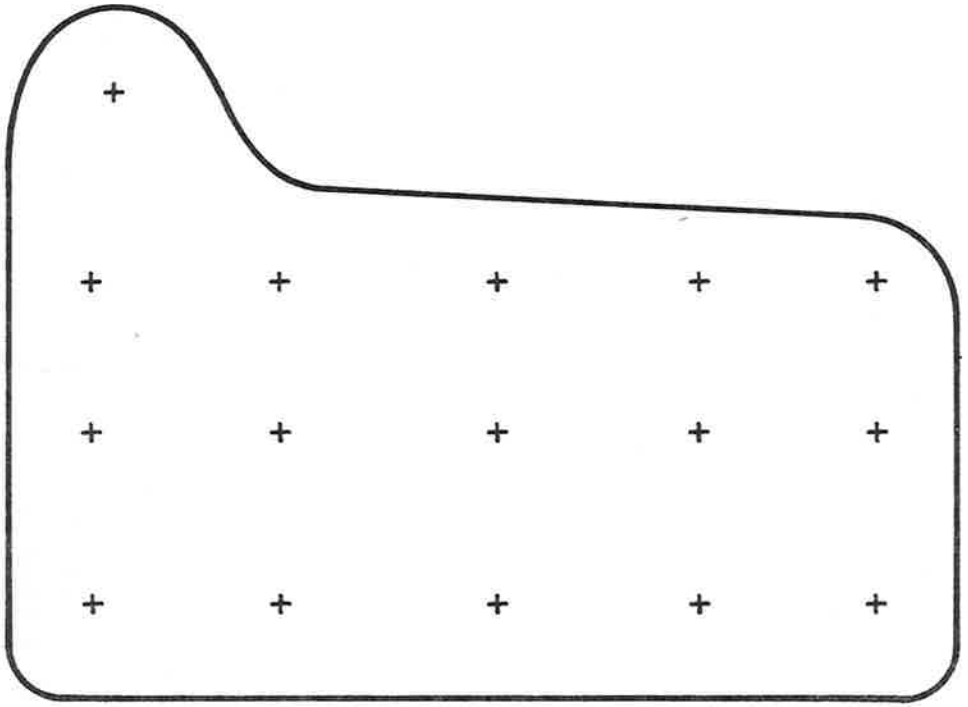

FIGURE 2. LOCATIONS OF BRINELL HARDNESS MEASUREMENTS ON RADIAL-AXIAL SECTIONS OF WHEEL RIMS (FULL SCALE)

TABLE 3. CONDITIONS FOR EMERGENCY-STOP BRAKING OF WHEEL NO. 1

Inertial wheel load	24,100 lb
Simulated car weight	192,800 lb
Brakeshoe arrangement and type	Single Cobra V-202
Brake force	7000 lb
Initial speed	130 mph (1210 rpm)
Kinetic energy per stop	13,670,000 ft-lb
Average stop time	87 sec
Average stop distance	8660 ft

Conversion Factors

1 lb = 0.225 N
1 mph = 1.61 km/hr
1 ft-lb = 1.36 J
1 ft = 0.305 m

pounds (107.2 kN), as close as was possible to 23,100 pounds, by using three large flywheels. A single flange-type composition brakeshoe (Cobra Type V-202, the same type used on Metroliner cars) was used for these tests. Brakeshoe force for the tests was 7000 pounds or 31.14 kN (as close as possible to the brake force of 6960 pounds or 30.96 kN used on Metroliner wheels). A translatory speed of 130 mph or 209 km/hr (1210 rpm for a 36-inch-diameter or 91-cm wheel) was selected for this test by DOT because this is the maximum anticipated speed of the Metroliner.

During stop testing, the wheel was initially rotated at 1210 rpm, and the brake was applied until the wheel stopped. Wheel speed, torque, work, stop time, equivalent stop distance, and brake force were continuously recorded and are summarized in Appendix B. Wheel temperature was not determined. After the wheel stopped, it was rotated at 20 rpm in air for 3 minutes, and then water sprays were directed toward the rotating rim for 10 minutes until the temperature of the wheel rim was reduced to ambient temperature. A total of 300 emergency stops were made. The wheel tread and flange were inspected periodically for thermal cracking by the fluorescent-magnetic-particle method.

2.3.2 Speed-Reduction-Braking Conditions for Wheel No. 2

The conditions for simulated speed-reduction braking of wheel No. 2, Table 4, were devised to be comparable to those of service speed-reduction braking. In this test, the single Cobra V-202 brakeshoe was applied with a force of 7000 pounds to slow the wheel from 930 rpm (100 mph or 161 km/hr) to 465 rpm (50 mph or 80 km/hr). After a period of 5 minutes, during which the speed was increased to 930 rpm, the brake was reapplied to reduce the speed to 465 rpm. After an additional 5-minute period and an increase of speed to 930 rpm, the brake was again reapplied to reduce the speed to 465 rpm. The wheel was then stopped dynamically* and cooled to ambient

*An exception was the first cycle in which the wheel was stopped with the brake.

TABLE 4. CONDITIONS FOR SPEED-REDUCTION BRAKING OF WHEEL NO. 2

Inertial wheel load	24,100 lb
Simulated car weight	192,800 lb
Brakeshoe arrangement and type	Single Cobra V-202
Brake force	7000 lb
Test cycle*	
Initial speed	100 mph (930 rpm)
Final speed	50 mph (465 rpm)
Kinetic energy per brake application	6,060,000 ft-lb
Average braking time	35 sec
Average braking distance	3800 ft

* The cycle was repeated three times at 5-minute intervals before the wheel was cooled to ambient temperature with water sprays.

Conversion Factors

1 lb = 0.225 N
1 mph = 1.61 km/hr
1 ft-lb = 1.36 J
1 ft = 0.305 m

temperature in the same manner as wheel No. 1. This cycle was repeated a total of 808 times (2,424 brake applications). The wheel rim was inspected frequently for thermal cracks by the fluorescent-magnetic-particle method, but none had developed. Data on torque, work, braking time, and wheel revolutions during braking are listed in Appendix C.

To assist in monitoring the simulated speed-reduction braking procedure, thermocouples were imbedded at the midwidth location of the wheel tread at depths of 1/16 and 1/4 inch (1.6 and 6 mm), as shown in Figure 3. In addition, duplicate strain gages (Micro-Measurements type WK-06-250BG-350) suitable for accurate strain measurements at temperatures up to 550°F (290°C) were oriented radially and cemented to the surface of the back-rim-plate fillet and front-hub-plate fillet, as shown in Figure 3. The thermocouples and strain gages were connected to appropriate measuring devices through a slip ring mounted on the stub axle. Selected temperatures and strains recorded during testing are listed in Appendix D.

2.3.3 Conditions for Braking of Wheel No. 3

Inasmuch as the results (to be discussed later) of the studies of the aforementioned dynamometer-tested wheels (Nos. 1 and 2) showed that thermal cracking and microstructural damage, such as observed in one of the used wheels (wheel No. 5), could not be produced by 300 simulated emergency-stop brakings or by 2424 simulated speed-reduction brakings, it was decided to subject wheel No. 3 to severe abnormal braking conditions, Table 5. First, the wheel was subjected to two drag-braking cycles to change the rim residual-stress condition from overall compression to overall tension. Each drag-braking cycle consisted of operation at a nominal speed of 419 rpm (45 mph or 72 km/hr) for 30 minutes and application of the brakeshoe with a force of 1900 pounds (8.45 kN) for 50 seconds of each minute. The rotating wheel was then cooled with water sprays until the temperature of the rim was at ambient. Next, the wheel was subjected to 10 emergency-stop braking cycles in an attempt to produce cracking, but none developed. (The

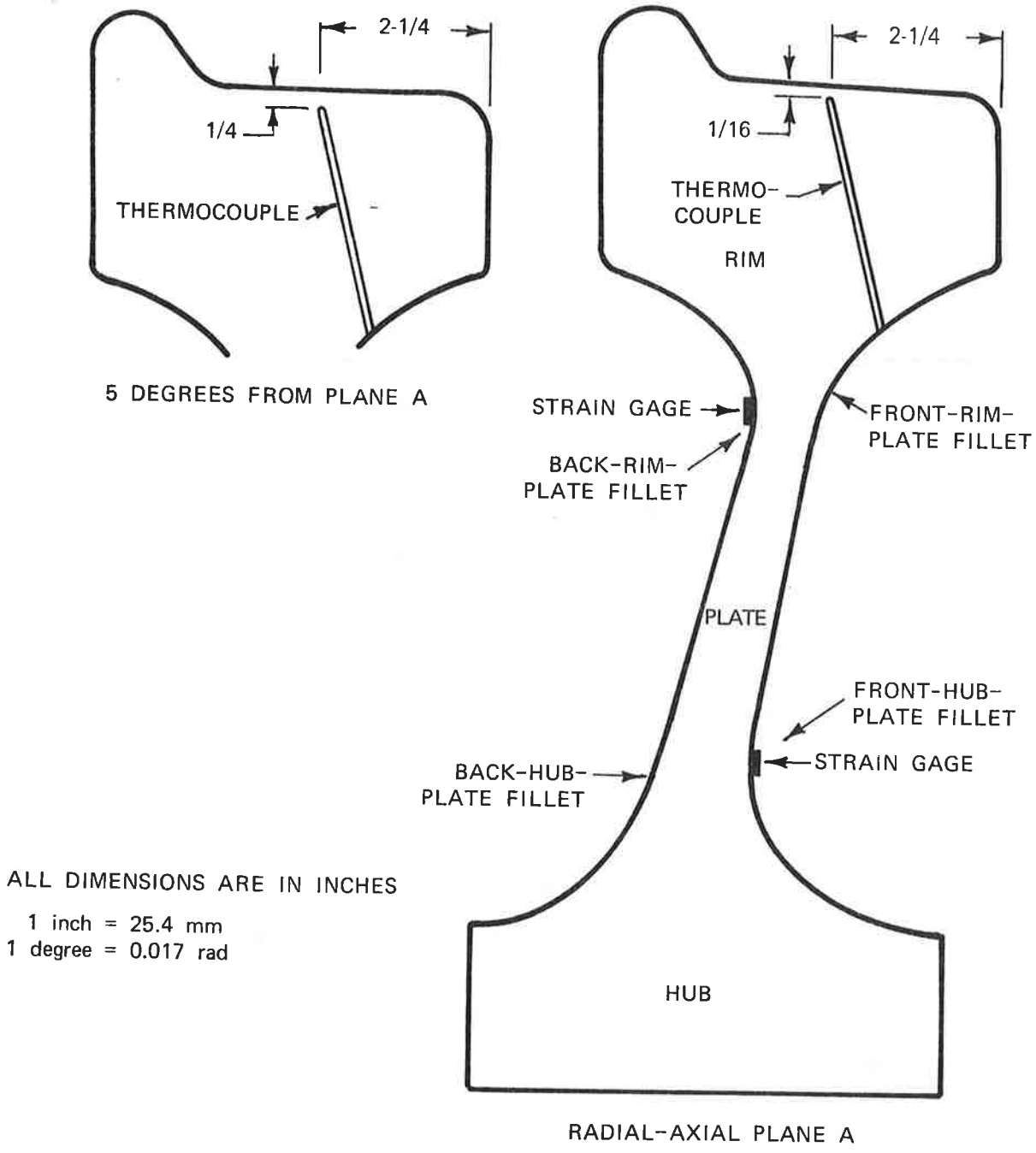

FIGURE 3. LOCATIONS OF THERMOCOUPLES AND STRAIN GAGES FOR DYNAMOMETER TESTS OF WHEEL NO. 2

TABLE 5. BRAKING CONDITIONS FOR WHEEL NO. 3

All Tests	
Inertial wheel load	24,100 lb
Simulated car weight	192,800 lb
Brakeshoe arrangement and type	Single Cobra V-202
Drag Braking	
Brake force*	1900 lb
Nominal speed**	419 rpm (45 mph)
Cooling	Water sprays on rim and plate
Emergency-Stop Braking* **	
Brake force	7000 lb
Initial speed	130 mph (1210 rpm)
Kinetic energy per stop	13,670,000 ft-lb
Average stop time	87 sec
Average stop distance	8660 feet
Cooling	Water sprays on rim and plate

* Braking for 50 seconds of each minute was continued for 30 minutes.

** Actually consisted of 100 rpm for 4 minutes, 200 rpm for 4 minutes, and 419 rpm for 22 minutes.

*** Seven stops were made with "wornout" shoes.

Conversion Factors

1 lb = 0.225 N
1 mph = 1.61 km/hr
1 ft-lb = 1.36 J
1 ft = 0.305 m

emergency-stop braking cycles were identical with those of wheel No. 1 except that water-spray cooling was started immediately after the wheel was stopped.) Two additional drag-braking cycles were then applied to produce higher hoop tensile stresses in the rim. Emergency-stop braking was then continued for 45 stops.

Because thermal cracks still had not developed, it was postulated that even more severe conditions, such as would occur by braking with a wornout brakeshoe, would be necessary to produce thermal cracking in the wheel. Accordingly, two brakeshoes were machined, as shown in Figure 4, so that only 1/4- and 1/8-inch (6 and 3 mm) thicknesses of composition material remained on the tread portion of the shoes. (The flange portion was cut off to facilitate machining of the tread portion.) The wheel was then subjected to seven emergency-stop braking cycles by using one of the machined brakeshoes. This resulted in a wearing away of about 80 percent of the composition material comprising the brakeshoe, Figure 4D. Using the second simulated wornout brakeshoe, the wheel was subjected to three additional emergency stops. As a result, the second brakeshoe exhibited worn-through areas and severe distortion, Figure 4E. These 10 emergency stops with simulated wornout brakeshoes produced discolored spots and deposits of backing-plate metal on the wheel tread surface. After the wornout brakeshoes were replaced with new shoes, emergency-stop braking was resumed for 45 additional stops. Small thermal cracks developed on the wheel tread surface during this period.

To assist in monitoring the tests on wheel No. 3 a thermocouple was placed in the rim, as shown in Figure 5. In addition, high-temperature strain gages (Micro-Measurements type WK-06-250WT-350) were cemented to the wheel surface at the back-rim-plate and front-hub-plate fillets, Figure 5. Static strain-gage measurements were taken after the wheel was cooled to determine whether the residual stresses at these locations were changed by the thermal cycles. Selected strain-gage and temperature data are listed in Appendix E, along with other pertinent data for this wheel.

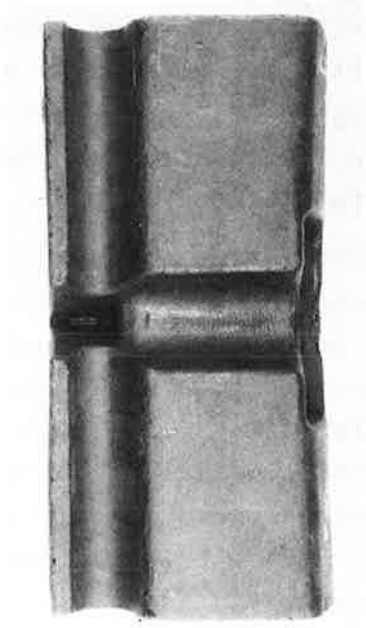

A. Front view—new shoe.

B. Side view—new shoe and simulated wornout shoe.

C. Front view—simulated wornout shoe.

D. Front view—First simulated wornout shoe after 7 stops.

E. Front view—Second simulated wornout shoe after 3 stops.

FIGURE 4. BRAKESHOE COMPOSITION (ABOUT 1/4X)

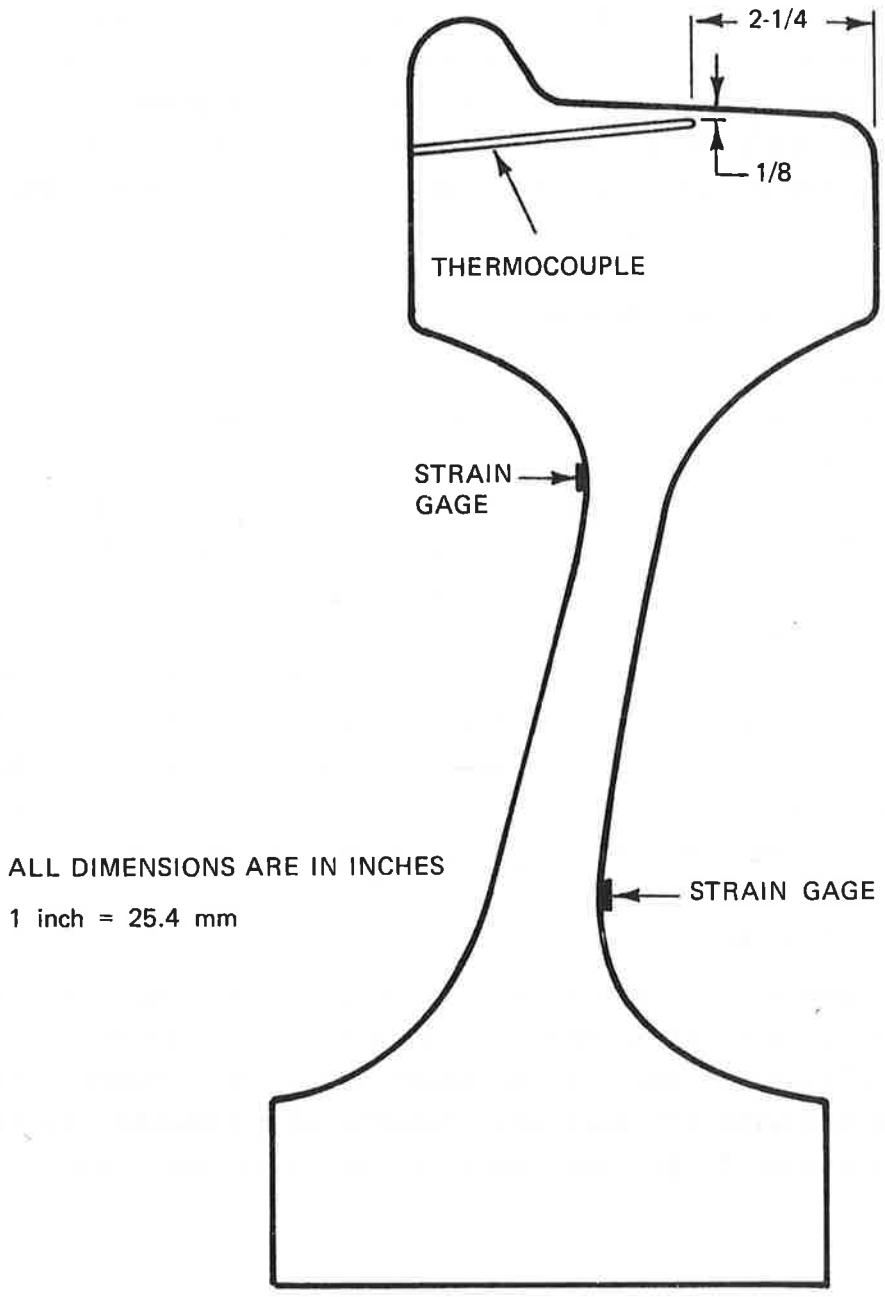

FIGURE 5. LOCATIONS OF THERMOCOUPLE AND STRAIN GAGES FOR DYNAMOMETER TESTS OF WHEEL NO. 3

2.4 RESIDUAL-STRESS STUDIES

Two stress-relaxation methods were used to determine residual stresses in the wheels. The overall residual hoop stresses in the rim were determined by the split-deflection method. The residual stresses at the rim surfaces and at the back-rim-plate fillet and the front-hub-plate fillet were determined by the dissection method. Figures 6 and 7 show the locations of gage marks and strain gages.

2.4.1 Split-Deflection Method

To measure the overall residual hoop stresses in the rim, pairs of gage marks, 2 inches (51 mm) apart on the tangential line 3/4 inch (19 mm) below the tread, were punched at axially opposite positions on the front and back faces of the rim (see Figure 6). The rim was then separated as a concentric section from the rest of the wheel by machining the inside circumference of the rim. A 1- to 1-1/2-inch-thick (25.4 to 38.1 mm) section was removed from between the gage marks. The change in distance between the gage marks was used to indicate the relative magnitude of the overall hoop stresses in the rim; an increase in gage distance (rim opening) indicated overall hoop tension, and a drcrease in gage distance (rim closure) indicated overall hoop compression.

2.4.2 Dissection Method

To measure the distribution of tangential residual stresses in the outer 1-inch-thick layer of the rim, single-element electrical-resistance foil strain gages (Micro-Measurements type EA-06-120AD-120 with 1/8-inch gage length) were cemented to the wheel-rim surfaces.* Several coatings (polyurethane varnish,

*Because the tread surface of wheel No. 2 was "grooved" to a depth of about 0.03 inch (0.76 mm) from brakeshoe action, the grooves were filled with Micro-Measurements AE-10, a 100-percent-solids epoxy system, before the gages were cemented. See Figures 10 and 20 for illustration of the grooves.

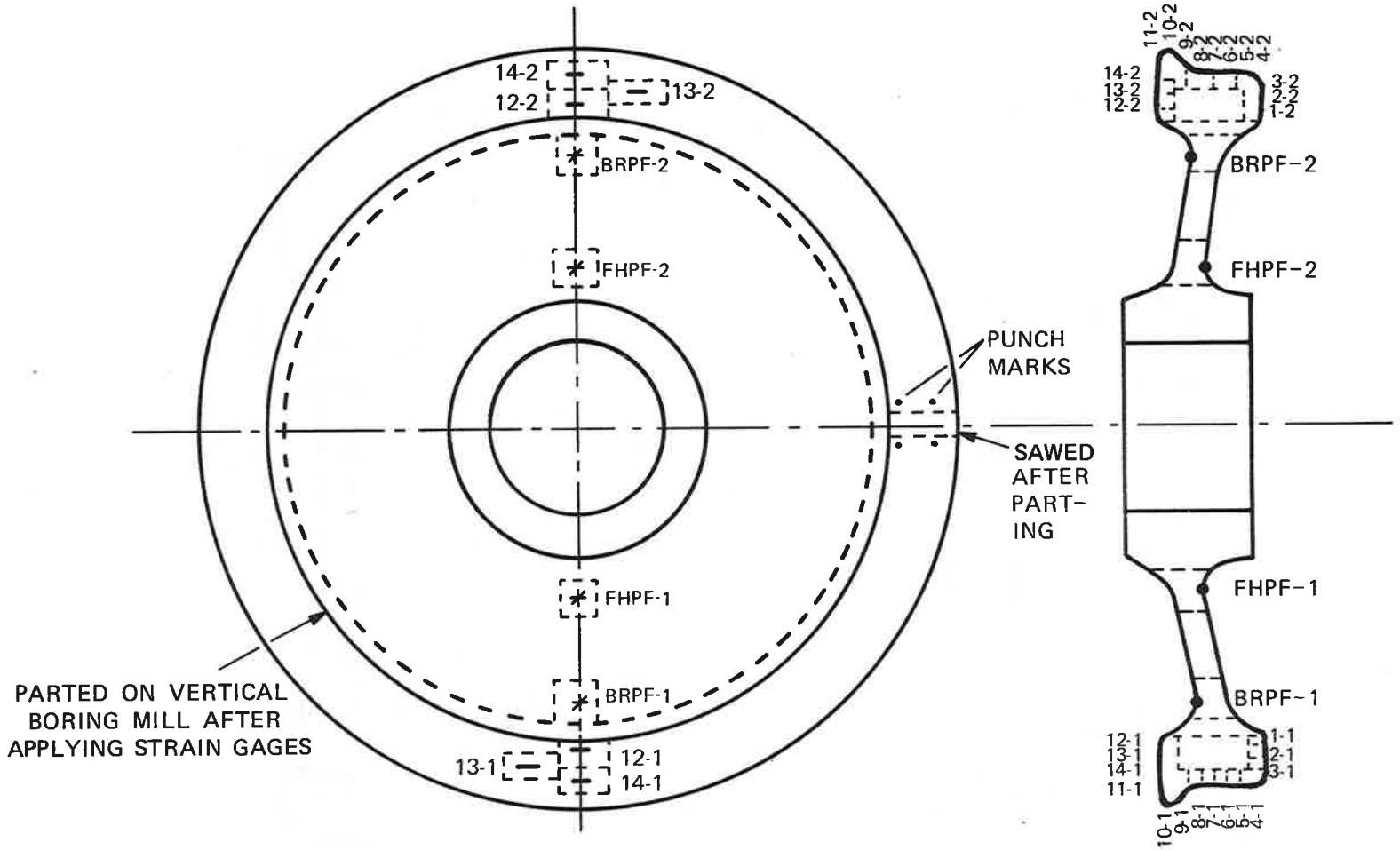

FIGURE 6. LOCATION OF STRAIN GAGES ON SECTION B-36 WHEEL

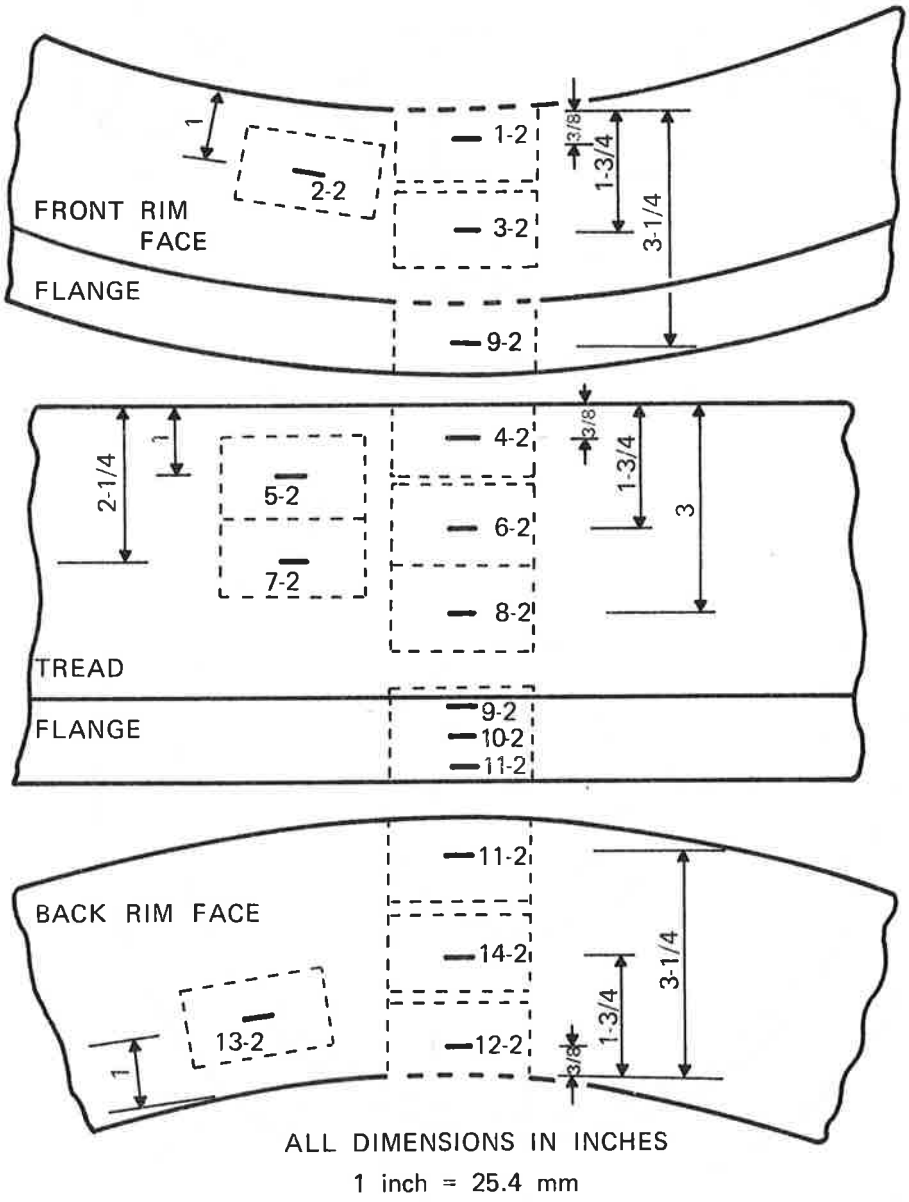

FIGURE 7. LOCATION OF STRAIN GAGES ON RIM OF SECTION B-36 WHEEL

silicone rubber, and steel sheet) were applied to the outside gage surface and to the adjacent steel surface to protect the gages from environmental and mechanical damage. After reference measurements of the strain gages were made, the wheel rim was dissected. Sections 1 inch square by 2 inches long with the strain gage on one surface were then saw-cut from the rim, and final measurements of the strain gages were made. Using the accepted value of 30 million psi (207 GPa) for Young's modulus, the tangential residual stresses were calculated from the relaxation strains (differences between the reference and final measurements of the strain gages).

The residual stresses at the bases of the back-rim-plate fillet and front-hub-plate fillet* were measured by means of 45-degree ($\pi/4$ rad) rectangular stacked-rosette electrical-resistance foil strain gages (Micro-Measurements type WA-06-250WR-120 with 1/4-inch gage length). The strain gages were cemented to the wheel plate and coated for environmental protection in the same manner as the rim gages. Before dissecting the wheel, reference measurements of the strain gages were made. Sections 2-1/2-inches (64 mm) square by plate thickness with the strain gages cemented to one surface were then sawed from the wheel, and the final measurements of the strain gages were made. The principal residual stresses were calculated from the measured relaxation strains, which are the differences between the reference and final strain-gage measurements.

The formulas for calculating the principal stresses are as follows:

*These locations are defined as the points on the plate-surfaces that have the greatest lateral distance from the back-rim face and the front-hub face.

$$S_{max} = \frac{E}{1-\mu}\left(\frac{e_r+e_t}{2}\right) + \frac{\sqrt{2}}{2}\left(\frac{E}{1+\mu}\right)\sqrt{(e_r - e_d)^2 + (e_d - e_t)^2}$$

$$S_{min} = \frac{E}{1-\mu}\left(\frac{e_r+e_t}{2}\right) - \frac{\sqrt{2}}{2}\left(\frac{E}{1+\mu}\right)\sqrt{(e_r - e_d)^2 + (e_d - e_t)^2}$$

where

e_r = strain in radial direction

e_t = strain in tangential direction

e_d = strain in 45° direction

E = Young's modulus (30×10^6 psi)

μ = Poisson's ratio (0.3)

3. RESULTS AND DISCUSSION

3.1 METALLURGICAL STUDIES

3.1.1 Chemical Composition

The chemical compositions of the six wheels are shown in Table 2, along with the specified range for AAR Specification M-107, Class A wheels. The chemical compositions of the wheels conformed to the specified ranges; however, their carbon contents (about 0.42%) were deliberately lower than typical (about 0.52%) for Class A wheels in order to improve their thermal-crack resistance and toughness.

3.1.2 Tensile Properties

The results of tension tests of 0.252-inch-diameter (6.4 mm) chordal specimens removed from the midthickness of the rims of the wheels are shown in Table 6. The tensile properties of the six wheels were similar to one another and were at levels that would be expected for rim-treated 0.4 percent carbon-steel wheels.

3.1.3 Impact Properties

The results of impact tests of chordal Charpy V-notch specimens from the midthickness of the rims of the wheels, Table 6, showed that the six wheels had essentially equivalent 50 percent shear-fracture-appearance temperatures, in the range 110 to 130°F (43 to 54°C). These values are normal for rim-toughened 0.4 percent carbon-steel sheels.

3.1.4 Hardness

The results of Brinell hardness tests of a cross section of each wheel rim, Table 7, showed that the hardnesses of the wheel rims were in the range expected for rim-treated 0.4 percent carbon-steel wheels.

TABLE 6. MECHANICAL PROPERTIES OF METROLINER WHEELS (CIRCUMFERENTIALLY ORIENTED SPECIMENS FROM THE RIMS)

Wheel No.	Tensile Properties				Impact Properties
	Yield Strength (0.2% Offset), ksi	Tensile Strength, ksi	Elongation in 1 Inch, percent	Reduction of Area, percent	50% Shear Temperature, °F
1*	64.6	110	20.0	48.2	+115
2*	67.6	112	21.5	45.4	+130
3*	70.5	110	21.0	45.3	+130
4**	71.3	112	20.0	46.2	+125
5***	73.6	113	20.0	47.0	+110
6****	66.3	108	21.5	49.9	+130

* After dynamometer tests.
** New.
*** Used - with thermal crack.
**** Used - no thermal crack.

Conversion Factors

1 ksi = 6.895 MPa
1 inch = 25.4 mm
°C = 5/9(°F - 32)

TABLE 7. BRINELL HARDNESS* OF RIMS OF METROLINER WHEELS

Wheel No. 1				
255				
255	241	241	241	255
229	217	217	217	241
207	212	207	217	207

Wheel No. 2				
269				
262	248	248	255	255
248	235	229	229	235
229	223	229	217	217

Wheel No. 3				
269				
225	241	269	269	269
241	229	223	223	229
223	212	207	207	207

Wheel No. 4				
262				
248	241	235	235	241
229	229	224	224	235
217	229	224	229	217

Wheel No. 5				
255				
241	241	285	285	285
229	229	229	235	255
217	217	229	229	235

Wheel No. 6				
255				
235	235	248	255	269
217	217	217	223	235
207	217	217	212	217

* Brinell hardness (Bhn) values are arranged as shown in Figure 2.

3.1.5 Visual Examination of Wheels

The tread of the untested new wheel (No. 4) exhibited no surface imperfections, as would be expected. The treads of both used wheels (No. 5 and 6) showed only a slight amount of wear, as would be expected from their short service period. Fluorescent magnetic-particle inspection, Figure 8, showed that wheel No. 5 had a 1-1/4-inch-long (32 mm) crack in the tread. The crack was oriented in the radial-axial plane. The appearance of the crack after being broken open in shown in Figure 9. It is apparent from the beach marks and oxidation that the crack was a fatigue-type thermal crack. The crack had a depth of about 3/16 inch (5 mm). Cracks were not present in the tread of wheel No. 6; neither wheel No. 5 nor wheel No. 6 exhibited cracks in the flange.

The tread of wheel No. 1 exhibited only slight grooving from brakeshoe-wheel interactions and no thermal cracks after 300 simulated emergency stops. As shown in Figure 10, wheel No. 2 had deep grooving on the tread but no thermal cracks on the tread or flange after 2,424 simulated speed-reduction brake applications. Wheel No. 3 exhibited slight grooving and several small thermal-fatigue cracks, Figure 11. As noted previously, these cracks developed during the emergency-stop braking which followed the braking with wornout brakeshoes.

3.1.6 Macrostructure and Microstructure

As shown in Figure 12, the macrostructure of the rim of the new wheel (No. 4) was uniform, and the microstructure consisted of fine pearlite with proeutectoid ferrite, principally at the prior-austenite grain boundaries, a normal microstructure for a new rim-treated 0.4 percent carbon-steel wheel.

Wheel No. 5, which exhibited a thermal crack developed in service, showed evidence of thermal damage from brakeshoe action. As shown in Figures 13 and 14, the tread of this wheel had been intermittently overheated along the circumference. The overheated regions had widths of about 3/4 inch (19 mm), lengths of from 1/2 to 1 inch (12 to 25 mm), and thicknesses of up to 0.06 inch (1.5 mm).

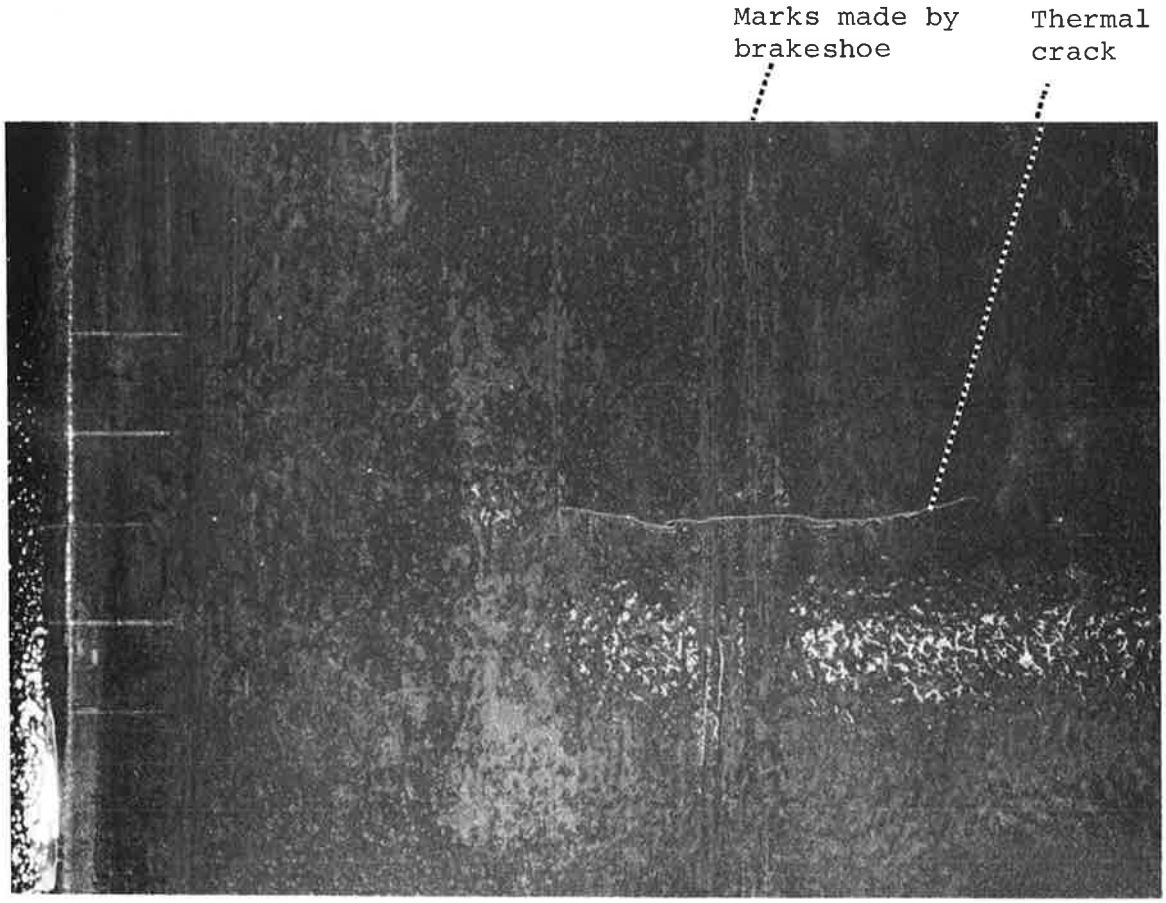

FIGURE 8. APPEARANCE OF THE TREAD SURFACE OF WHEEL NO. 5, SHOWING A THERMAL CRACK AS REVEALED BY FLUORESCENT MAGNETIC-PARTICLE INSPECTION. SCRIBNER MARKS ON CORNER OF TREAD WERE USED FOR REFERENCE FOR NONDESTRUCTIVE TESTS CONDUCTED BY OTHER CONTRACTORS (ABOUT 2X)

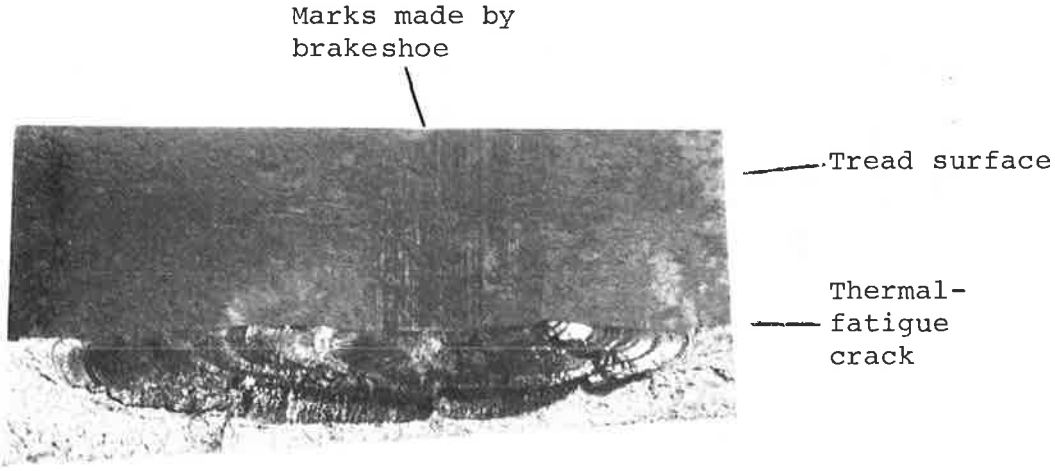

FIGURE 9. THERMAL-FATIGUE CRACK IN WHEEL NO. 5 AFTER BEING BROKEN OPEN (ABOUT 3X)

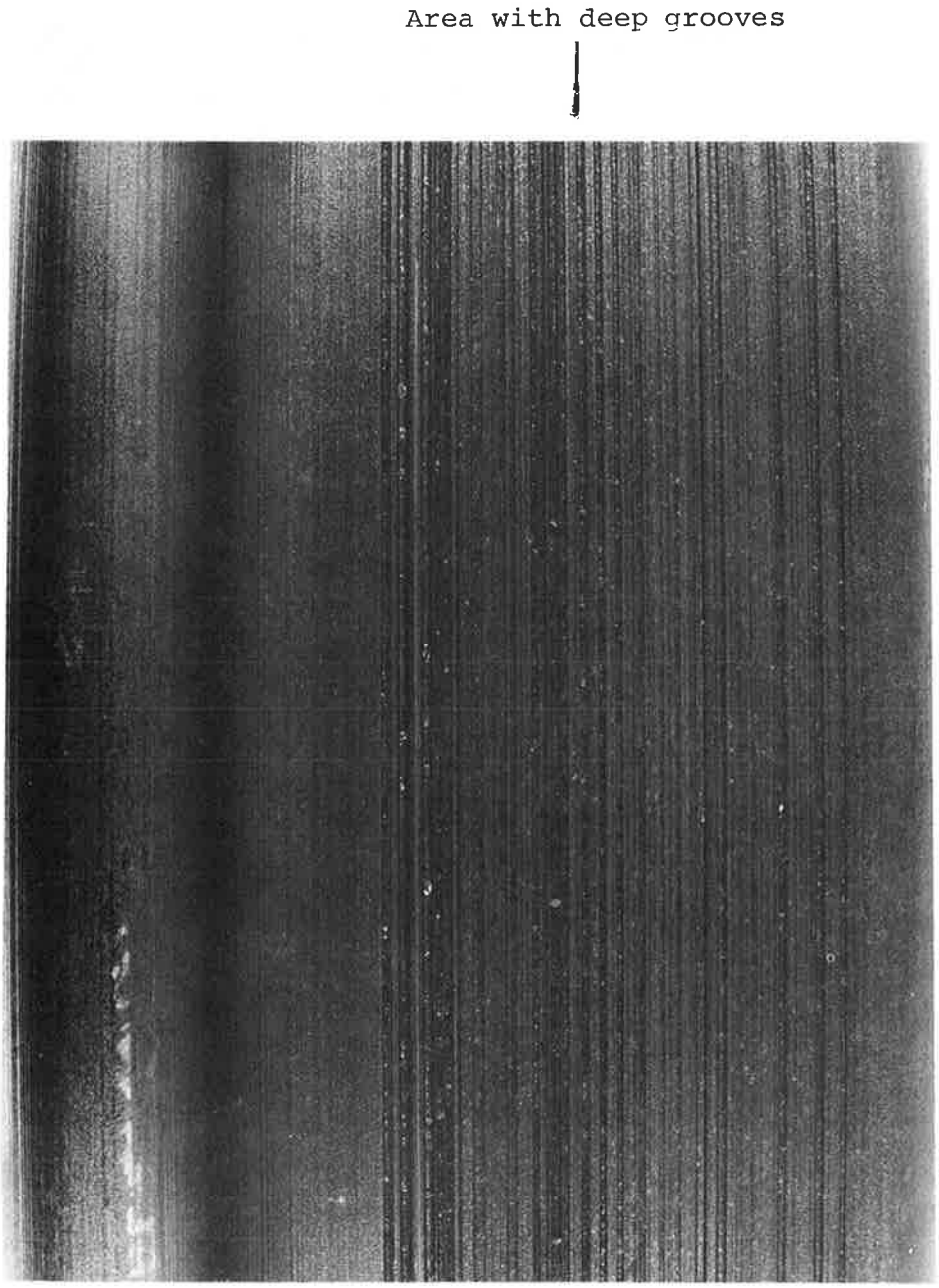

FIGURE 10. APPEARANCE OF TREAD AND FLANGE OF WHEEL NO. 2 AFTER SPEED-REDUCTION BRAKE TESTING. NOTE GROOVES CAUSED BY BRAKE-SHOE-WHEEL INTERACTION (ACTUAL SIZE - SEE FIG. 20 FOR ILLUSTRATION OF GROOVE DEPTH)

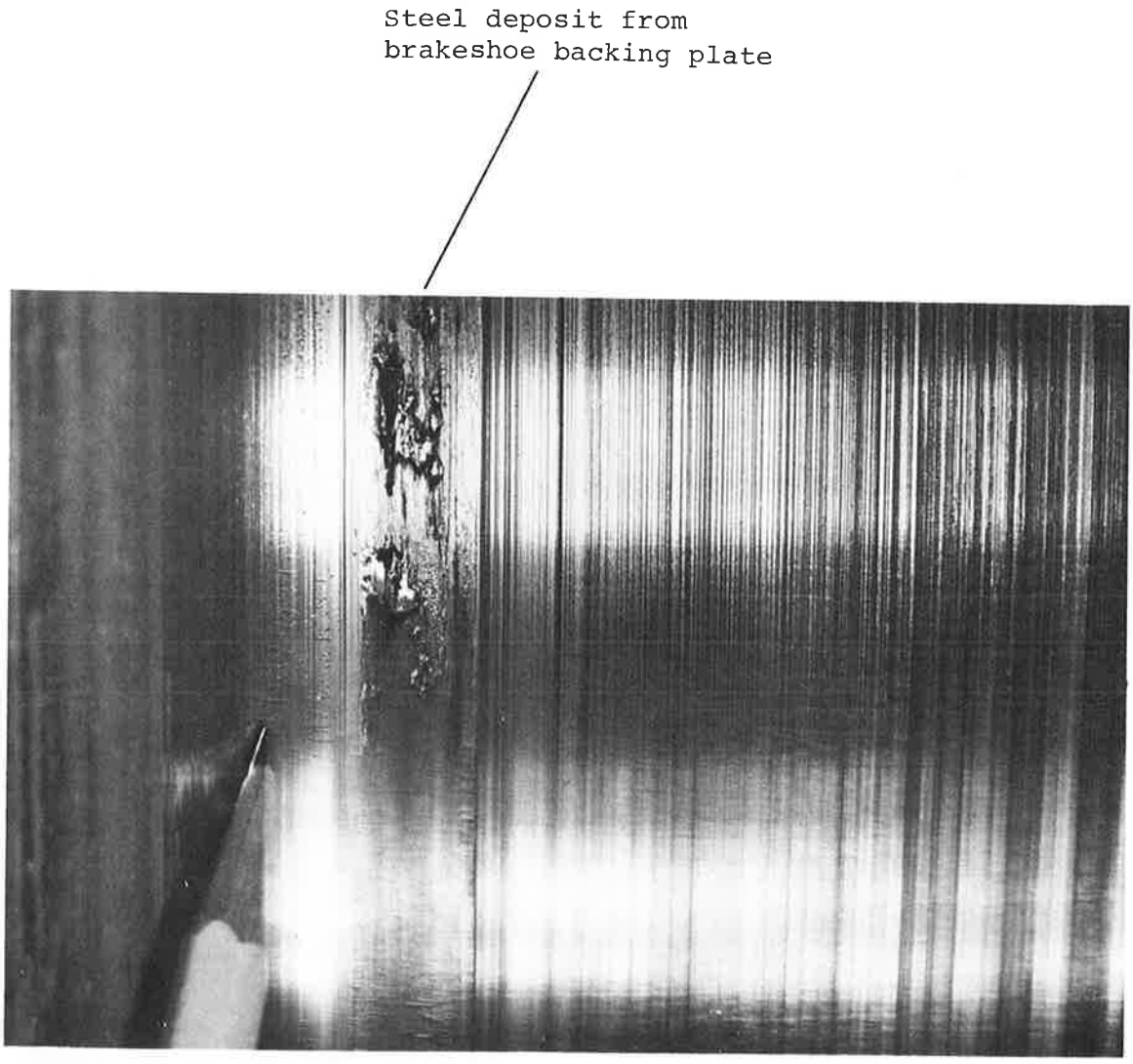

FIGURE 11. APPEARANCE OF TREAD OF WHEEL NO. 3 AFTER TESTING ON WHEEL-TEST MACHINE (DRAG BRAKING AND EMERGENCY-STOP BRAKING WITH WORNOUT BRAKESHOES). THE PENCIL POINTS TO SEVERAL SMALL THERMAL-FATIGUE CRACKS (ABOUT 2X)

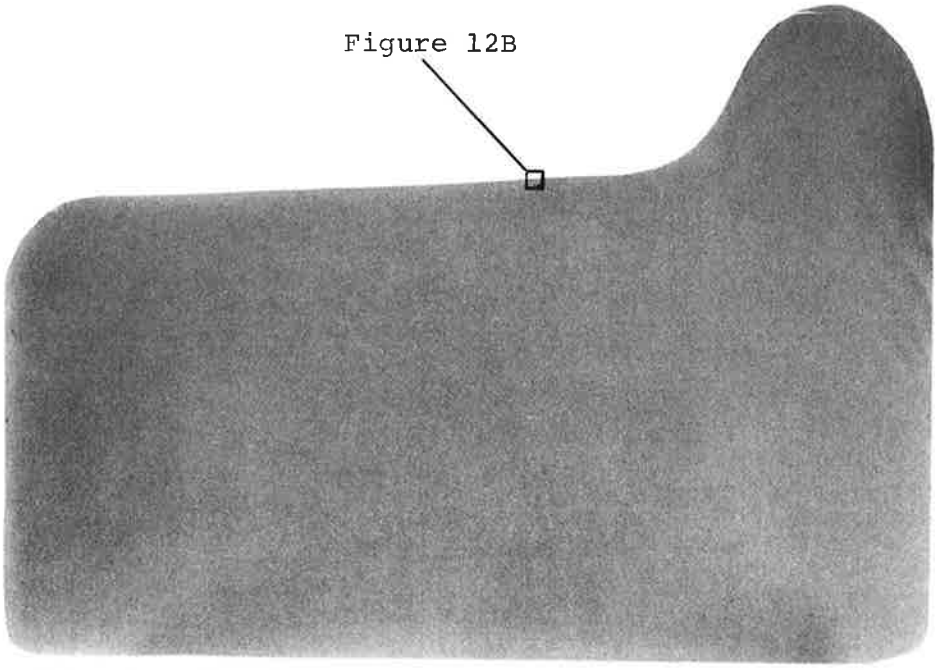

A. Macrostructure of radial-axial section. Nital etch. Actual size

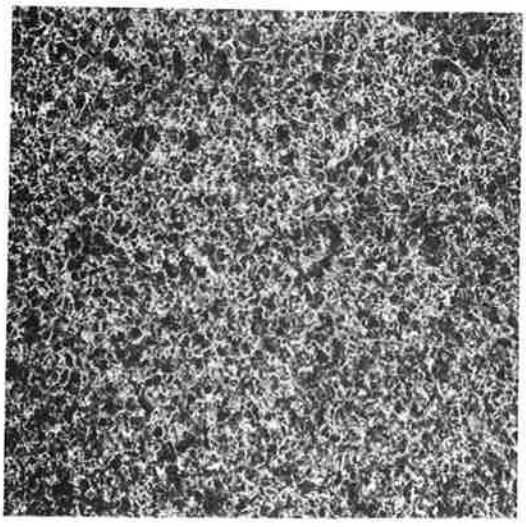

B-1. 300 dph. X50.

B-2. 300 dph. X500.

B. Microstructure and microhardness of tread. Superpicral etch.

FIGURE 12. MACROSTRUCTURE, MICROSTRUCTURE, AND MICROHARDNESS OF RADIAL-AXIAL SECTION OF RIM OF WHEEL NO. 4 (NEW AND UNTESTED)

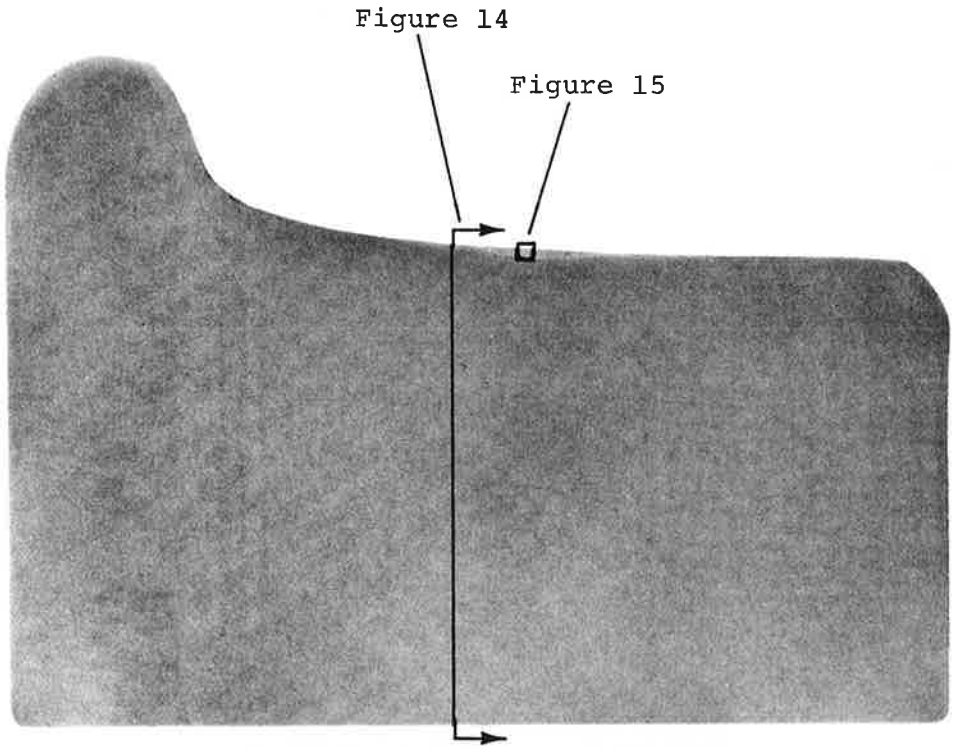

FIGURE 13. MACROSTRUCTURE OF RADIAL-AXIAL SECTION OF RIM OF WHEEL NO. 5, SHOWING LIGHT-ETCHING STRUCTURE RESULTING FROM TREAD OVERHEATING. NITAL ETCH (ACTUAL SIZE)

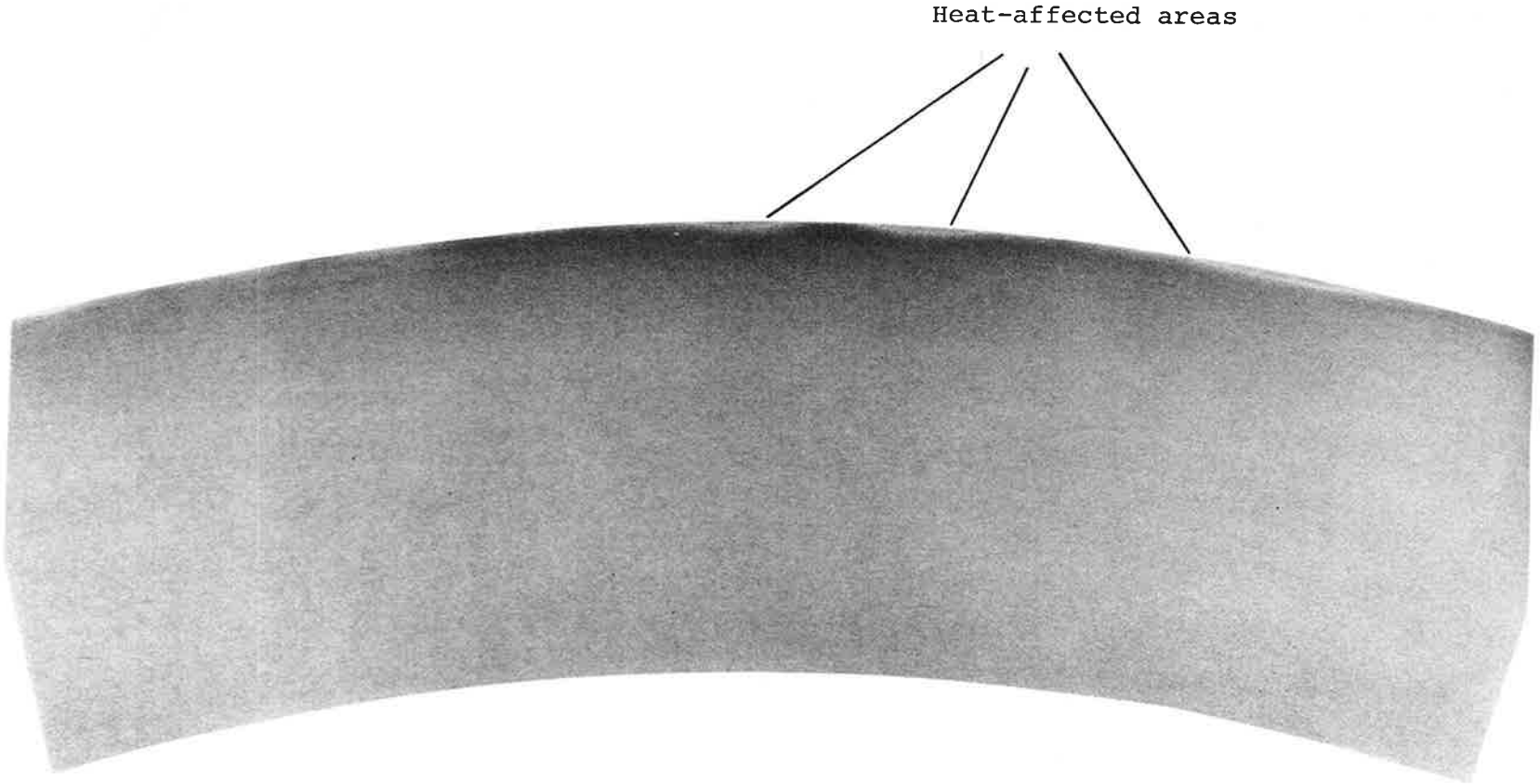

FIGURE 14. MACROSTRUCTURE OF RADIAL-TANGENTIAL SECTION OF RIM OF WHEEL NO. 5, SHOWING LIGHT-ETCHING STRUCTURE RESULTING FROM OVERHEATING OF TREAD. NITAL ETCH (ACTUAL SIZE)

These regions were randomly spaced around the circumference of the tread at intervals of from 1 to 4 inches (25 to 100 mm) at a distance of 2 to 3 inches (50 to 75 mm) from the front face of the rim. Figure 15 shows the range of microstructures obtained in one such heat-affected area. Most of the heat-affected area consisted of a very-fine-grained gerrite-pearlite microstructure. The transition zone, which had a thickness of about 0.005 inch (0.13 mm), consisted of ferrite and partially spheroidized pearlite with the same grain size as the unaltered ferrite-pearlite of the remainder of the rim. The microhardnesses of these microstructures were all about 300 dph. The thermal-fatigue crack (Figure 9) had initiated in one of these overheated areas. On the basis of the microstructural studies of wheel No. 5, it is estimated that the tread surface was heated to a high enough temperature (above 1333°F or 723°C) to cause reaustenitization, but the cooling rate was insufficient to result in the formation of hard and brittle martensite. In contrast, Figures 16 and 17 show that the macrostructure of the rim of used wheel No. 6 was uniform and devoid of "heat-affected" areas. Furthermore, microstructure examinations, Figure 18, of areas near the tread surface of wheel No. 6 showed ferrite and pearlite; there was no evidence of overheating.

On the basis of these studies, it is concluded that wheel No. 5 had been overheated by brakeshoe action while in service and that the mate wheel (No. 6) had not. Such unequal braking conditions are possible inasmuch as the two wheels were independently braked. Because it was suspected that wheel No. 5 had been braked with wornout brakeshoes, causing the overheating and "hot" spots observed, simulated wornout brakeshoes were used in the final series of dynamometer tests performed on wheel No. 3 to test this hypothesis.

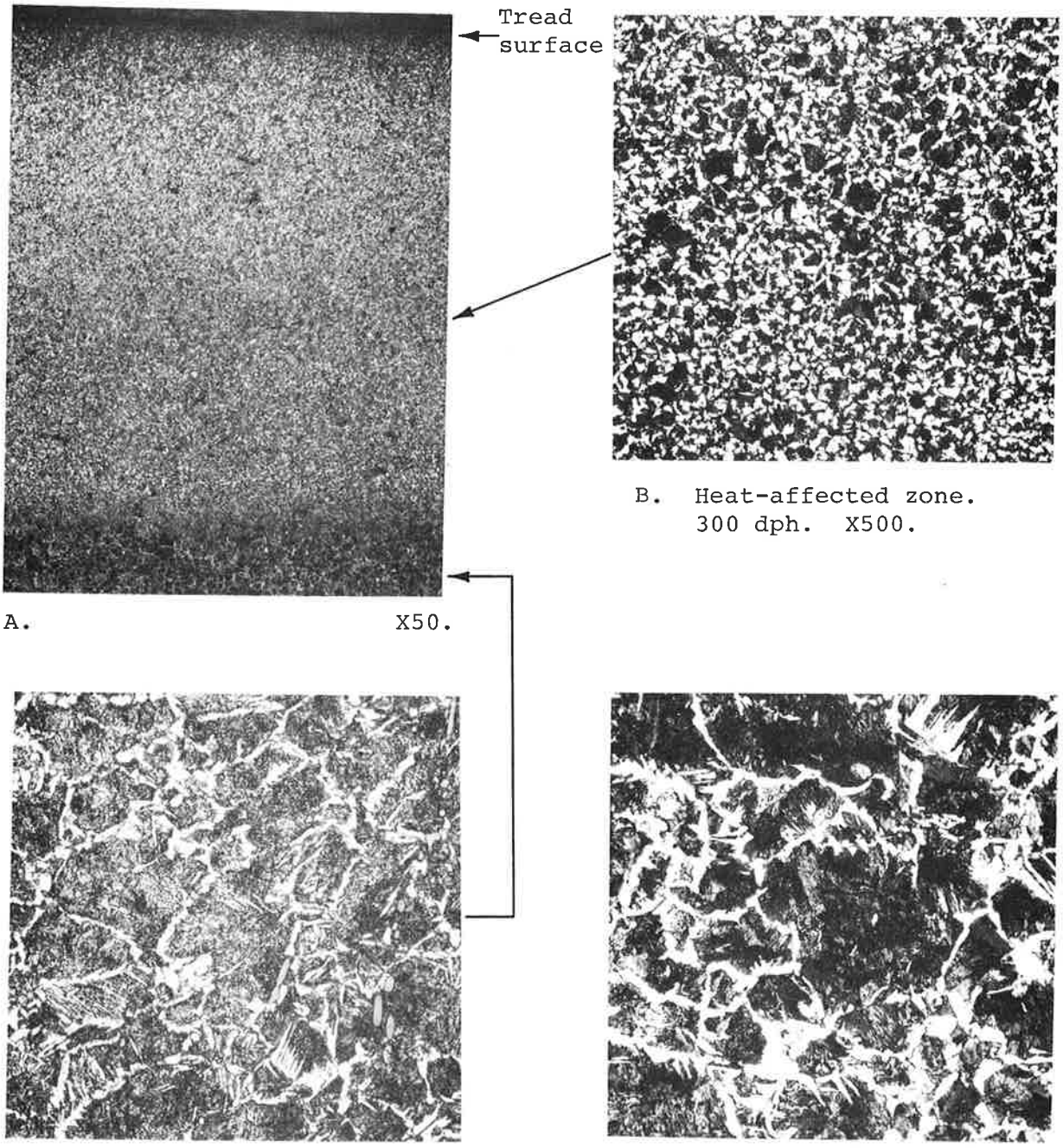

A. X50.

B. Heat-affected zone. 300 dph. X500.

C. Transition zone. 280 dph. X500.

D. Unaltered metal. 300 dph. X500.

FIGURE 15. MICROSTRUCTURE AND MICROHARDNESS OF RADIAL-AXIAL SECTION OF RIM OF WHEEL NO. 5 THROUGH HEAT-AFFECTED AREA. SUPER-PICRAL ETCH

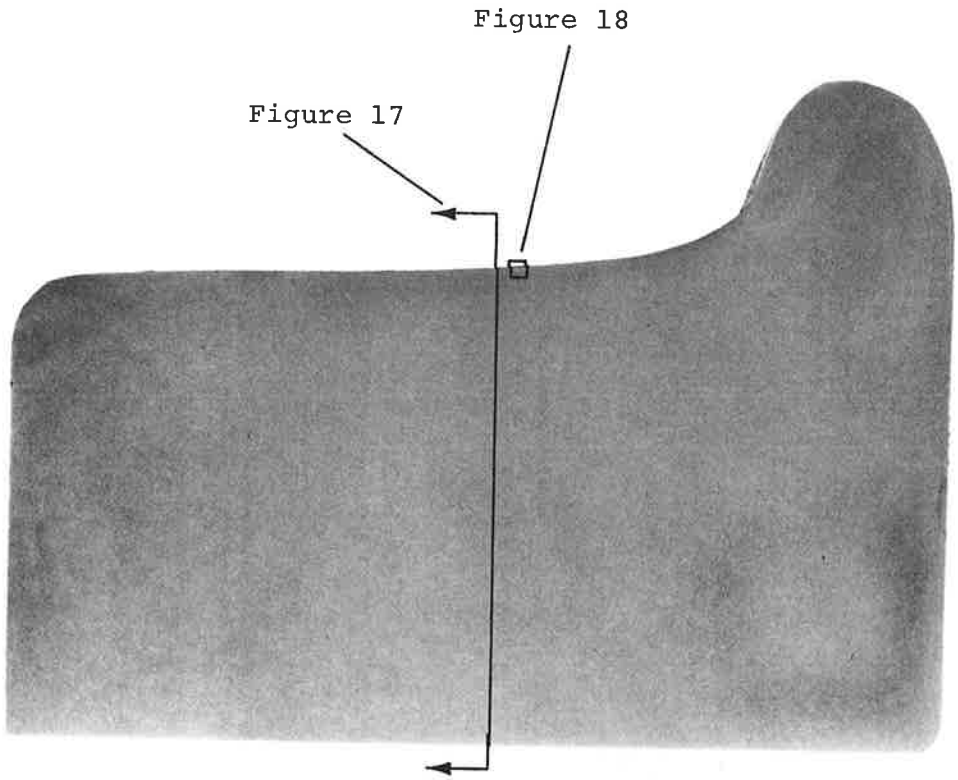

FIGURE 16. MACROSTRUCTURE OF RADIAL-AXIAL SECTION OF RIM OF WHEEL NO. 6. NITAL ETCH (ACTUAL SIZE)

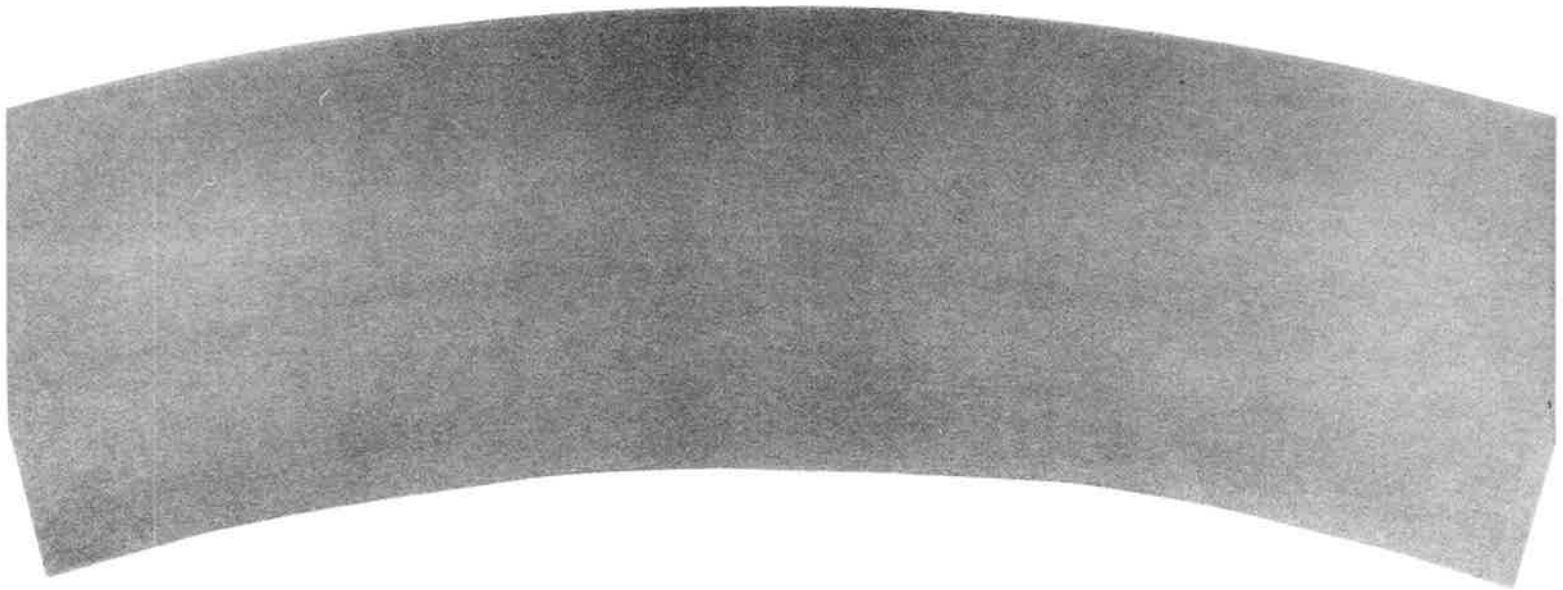

FIGURE 17. MACROSTRUCTURE OF RADIAL-TANGENTIAL SECTION OF RIM OF WHEEL NO. 6. NITAL ETCH (ACTUAL SIZE)

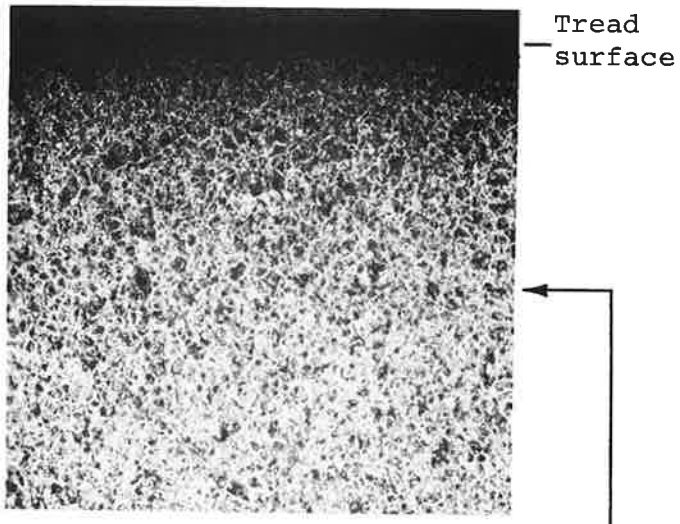

A. 300 dph X50.

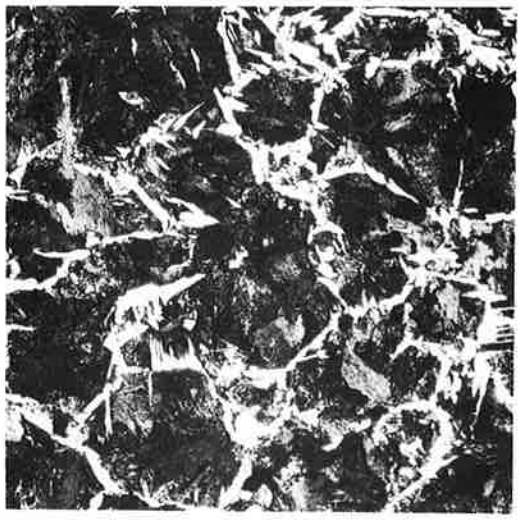

B. 300 dph X50.

FIGURE 18. MICROSTRUCTURE AND MICROHARDNESS OF RADIAL-AXIAL SECTION OF TREAD OF WHEEL NO. 6. SUPER-PICRAL ETCH

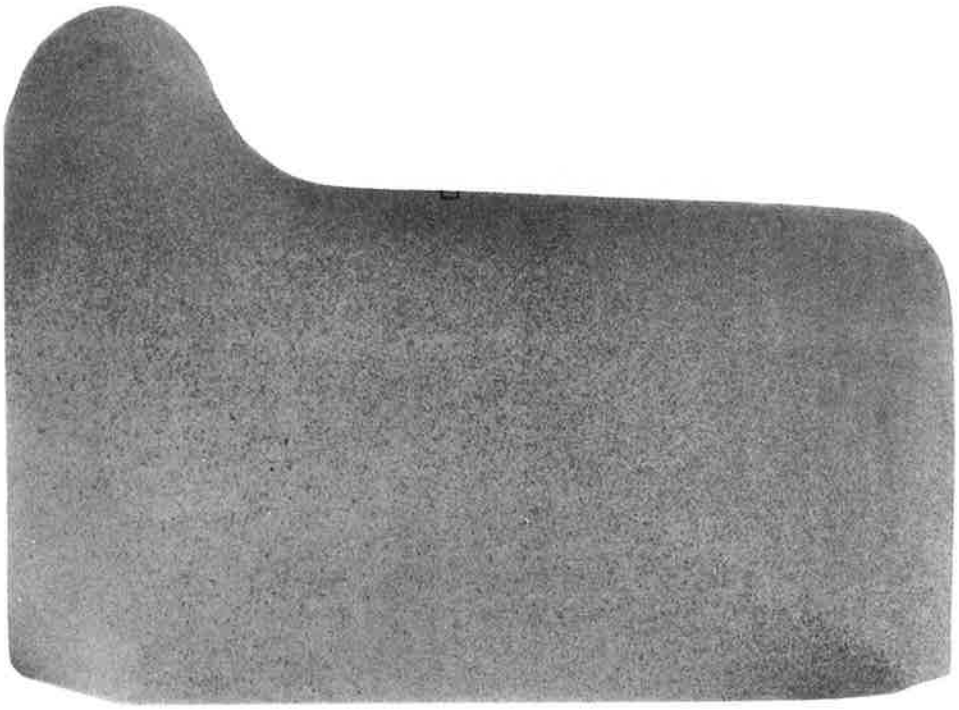

A. Macrostructure of radial-axial section. Nital etch. Actual size.

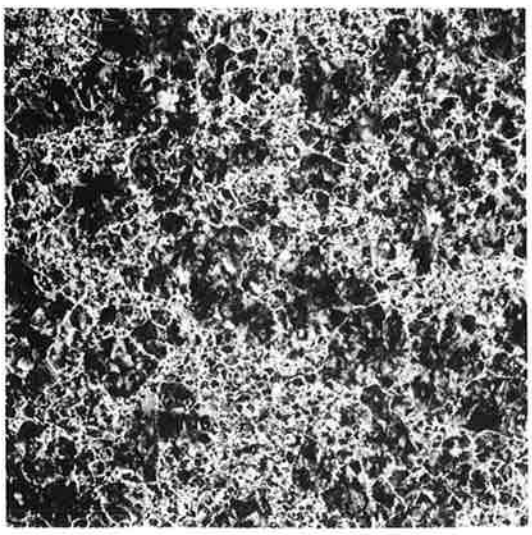

Tread surface

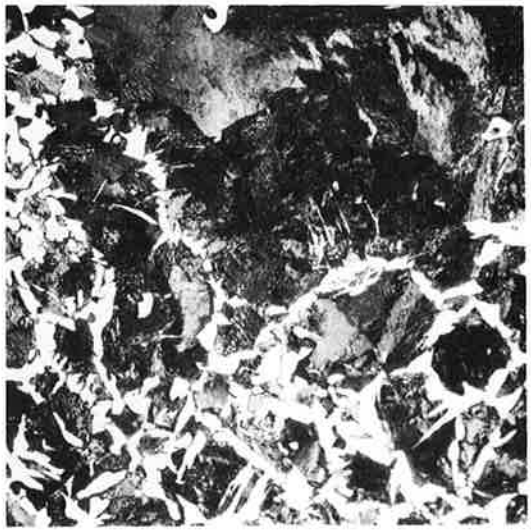

B-1. 300 dph. X50. B-2. 300 dph. X500.

B. Microstructure of radial-axial section at tread center. Super-picral etch.

FIGURE 19. MACROSTRUCTURE, MICROSTRUCTURE, AND MICROHARDNESS OF RADIAL-AXIAL SECTION OF RIM OF WHEEL NO. 1

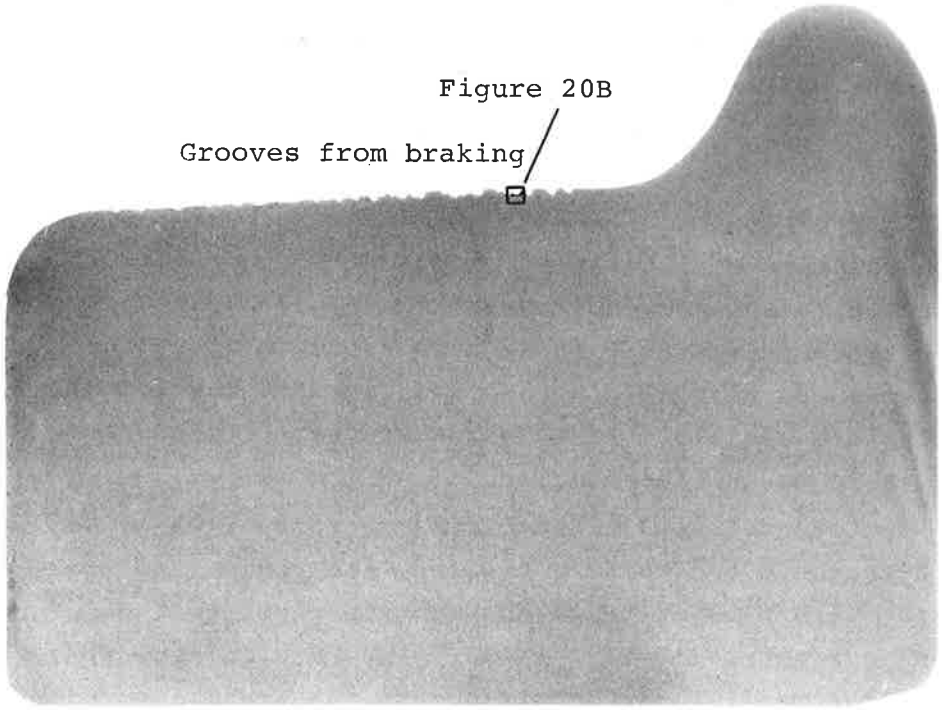

A. Macrostructure of radial-axial section. Nital etch. Actual size.

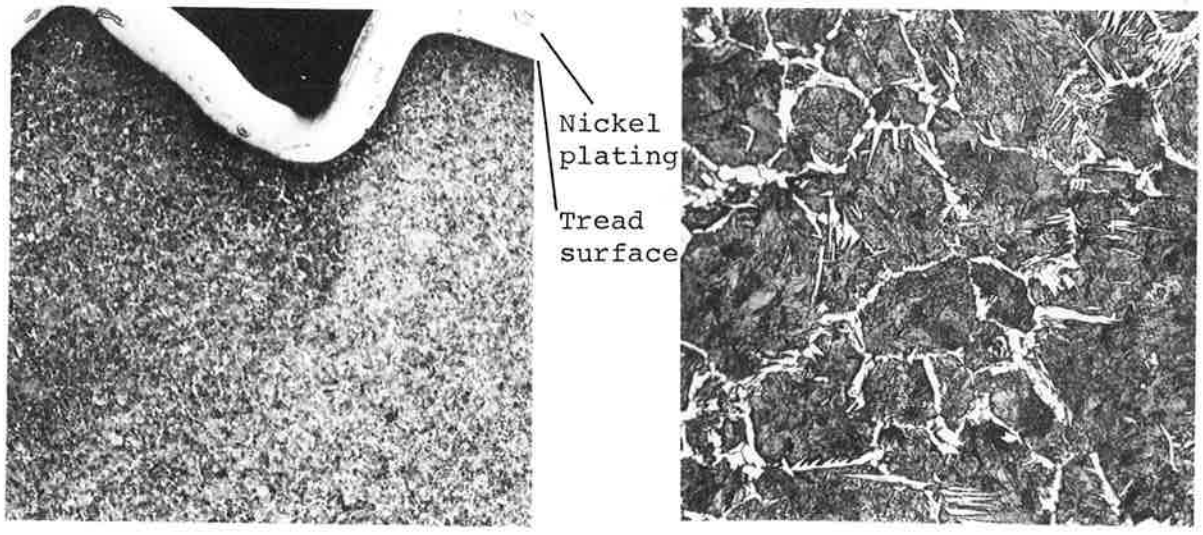

B-1. 300 dph. X50. B-2. 300 dph. X500.

B. Microstructure of tread. Super-picral etch

FIGURE 20. MACROSTRUCTURE, MICROSTRUCTURE, AND MICROHARDNESS OF RADIAL-AXIAL SECTION OF RIM OF WHEEL NO. 2

Figure 19 shows the macrostructure and microstructure of the rim of wheel No. 1 after 300 simulated emergency stops. No evidence of thermal damage caused by braking was detected in the macrostructure. The microstructure near the tread consisted of fine pearlite with proeutectoid ferrite at the prior-austenite grain boundaries. Figure 20 shows the macrostructure and microstructure of the rim of wheel No. 2, the wheel that had been subjected to speed-reduction braking on the dynamometer. The macrostructure was uniform with no evidence of overheating near the tread and flange. In addition, the grooves resulting from braking are visible. Examination of the microstructure confirmed that there was no overheating.

The macrostructure and microstructure of wheel No. 3, which had been subjected to drag braking, emergency-stop braking, and braking with wornout brakeshoes on the wheel-test machine, are shown in Figures 21, 22, and 23. The results show that this wheel was overheated intermittently around the tread circumference in much the same manner as wheel No. 5. The microstructure and size of these overheated areas, Figure 23, were similar to those in wheel No. 5, Figure 15.

3.2 RESIDUAL STRESSES

Data from the residual-stress studies are listed in Appendixes F and G and summarized in Figures 24 through 29.

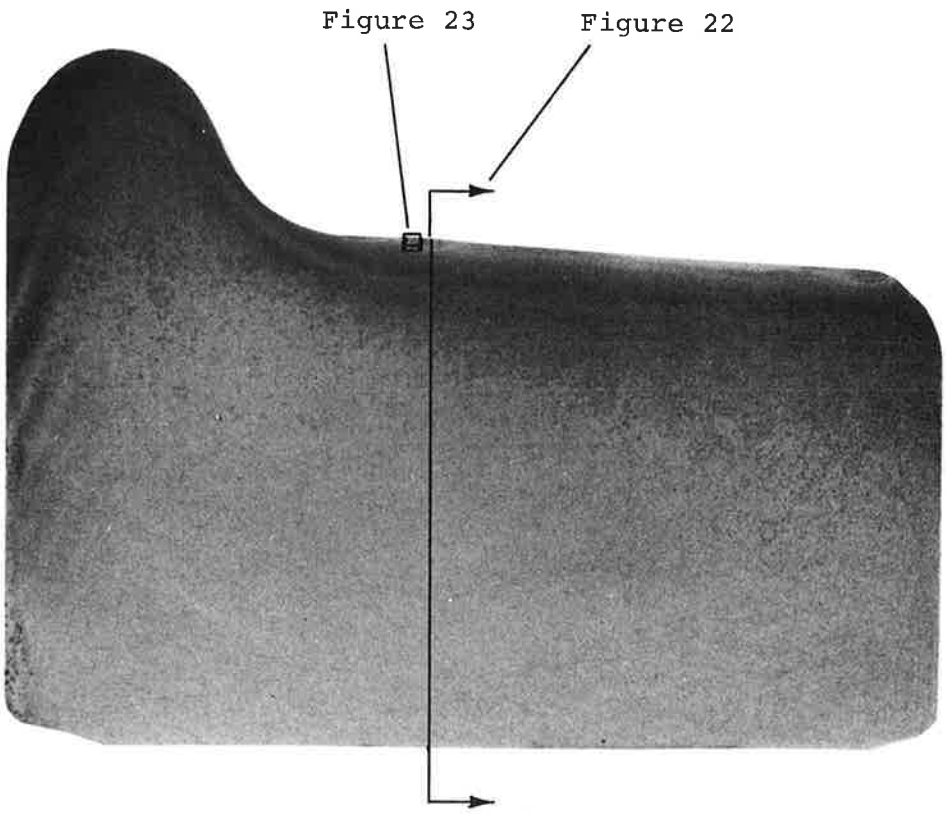

FIGURE 21. MACROSTRUCTURE OF RADIAL-AXIAL SECTION OF RIM OF WHEEL NO. 3, SHOWING LIGHT-ETCHING "HEAT-AFFECTED" AREA ON TREAD. NITAL ETCH (ACTUAL SIZE)

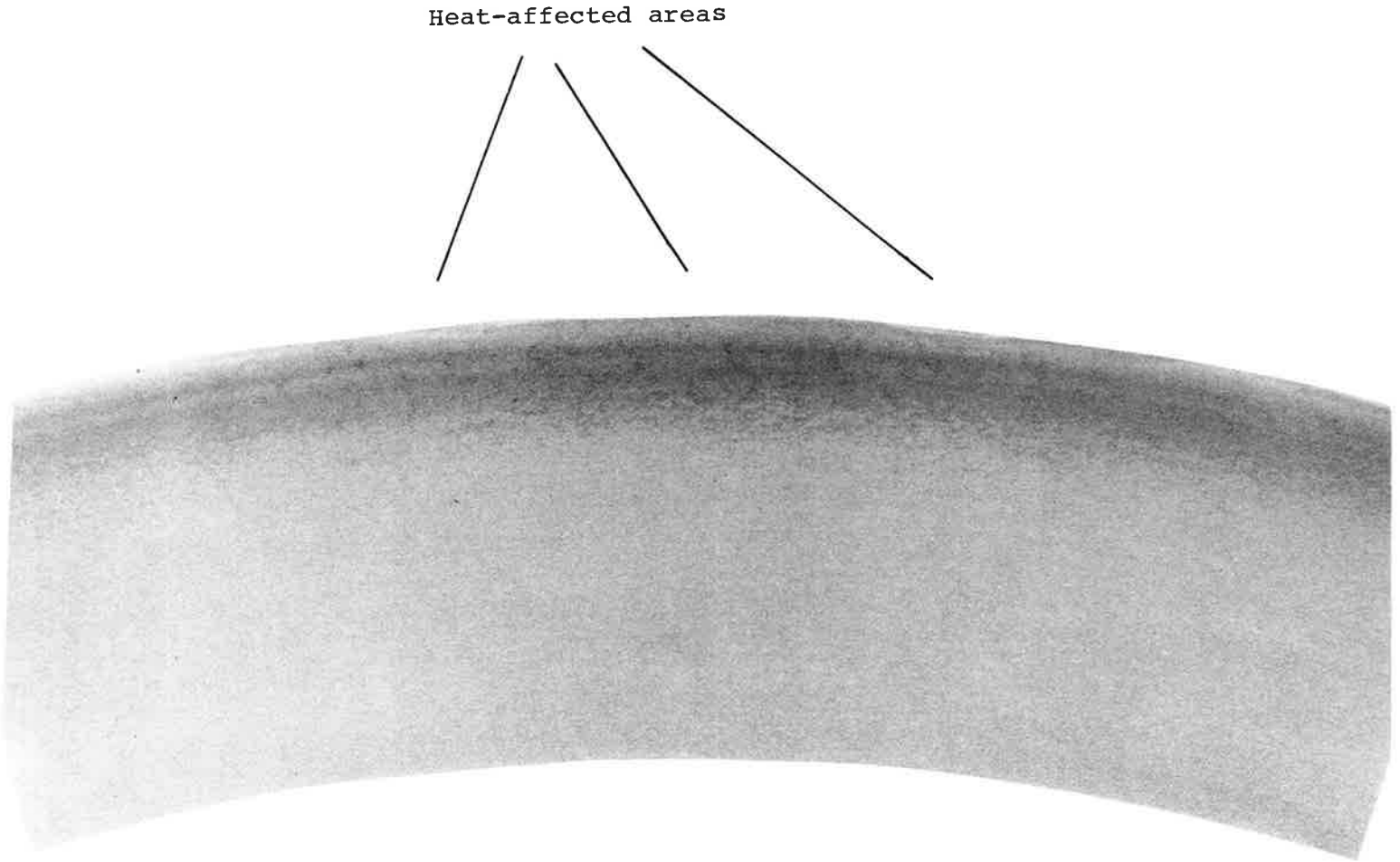

FIGURE 22. MACROSTRUCTURE OF RADIAL-TANGENTIAL SECTION OF RIM OF WHEEL NO. 3, SHOWING LIGHT-ETCHING "HEAT-AFFECTED" AREA ON TREAD. NITAL ETCH (ACTUAL SIZE)

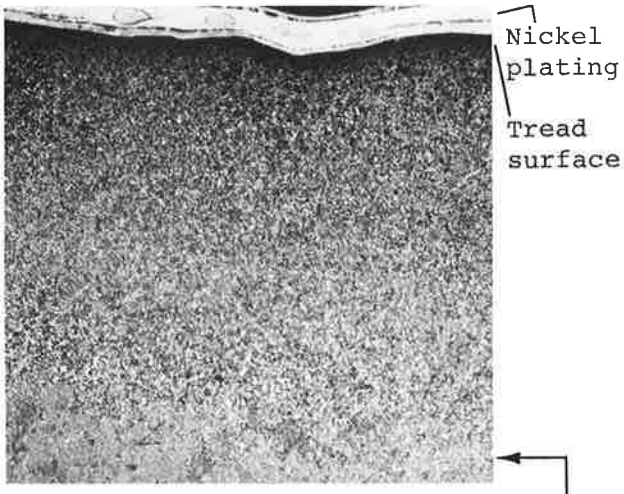

A. X50.

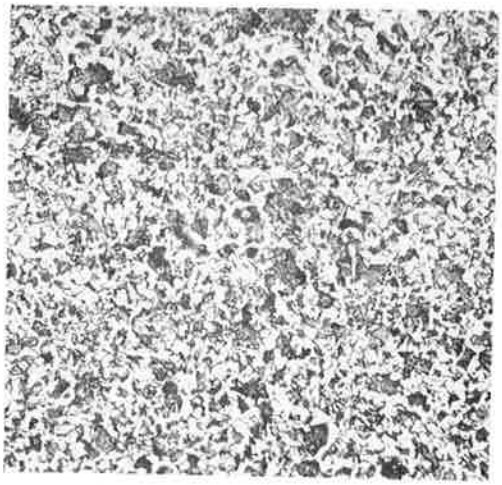

B. Heat-affected zone. 300 dph. X500.

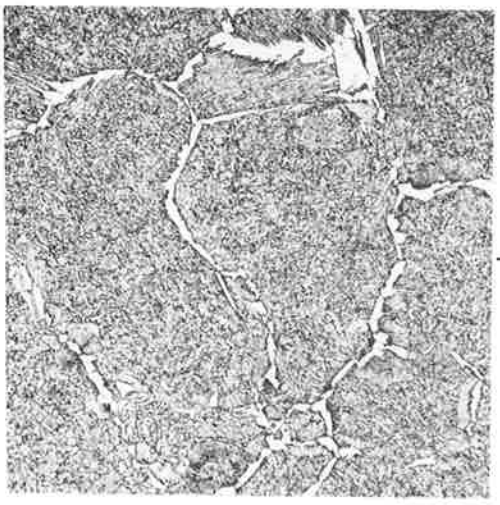

C. Transition zone. 280 dph. X500.

D. Unaltered metal. 300 dph. X500.

FIGURE 23. MICROSTRUCTURE AND MICROHARDNESS OF RADIAL-AXIAL SECTION OF RIM OF WHEEL NO. 3 THROUGH HEAT-AFFECTED AREA. SUPER-PICRAL ETCH

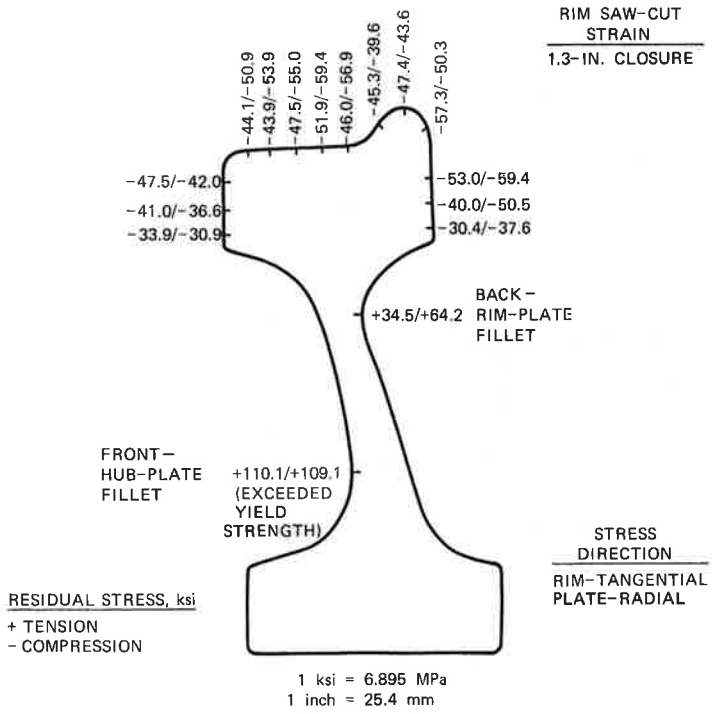

FIGURE 24. INDICATED RESIDUAL STRESSES IN NEW WHEEL NO. 4 (1-72-S-2466-A)

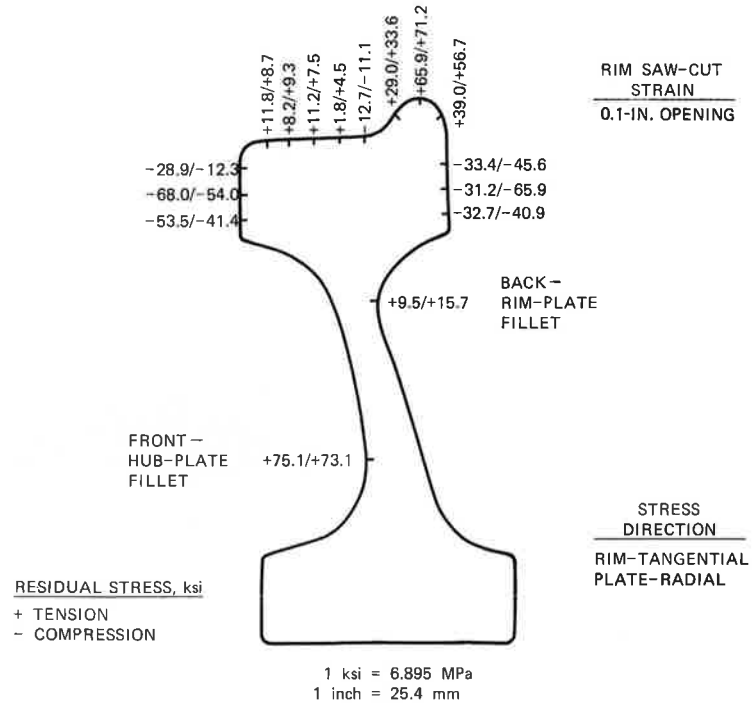

FIGURE 25. INDICATED RESIDUAL STRESSES IN USED WHEEL NO. 5 (1-71-S-10191-A) WHICH CONTAINED FATIGUE-TYPE THERMAL CRACK

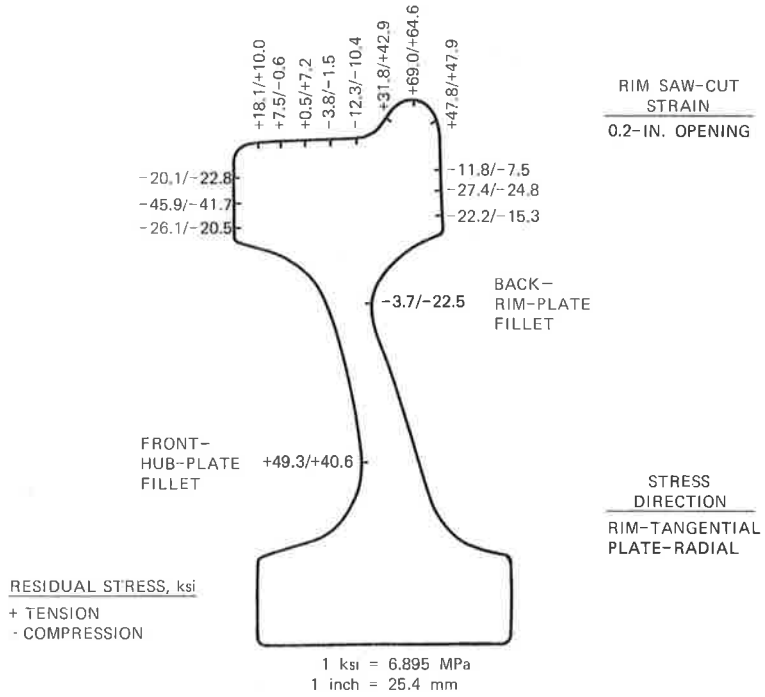

FIGURE 26. INDICATED RESIDUAL STRESSES IN USED WHEEL NO. 6 (1-71-S-10190-A)

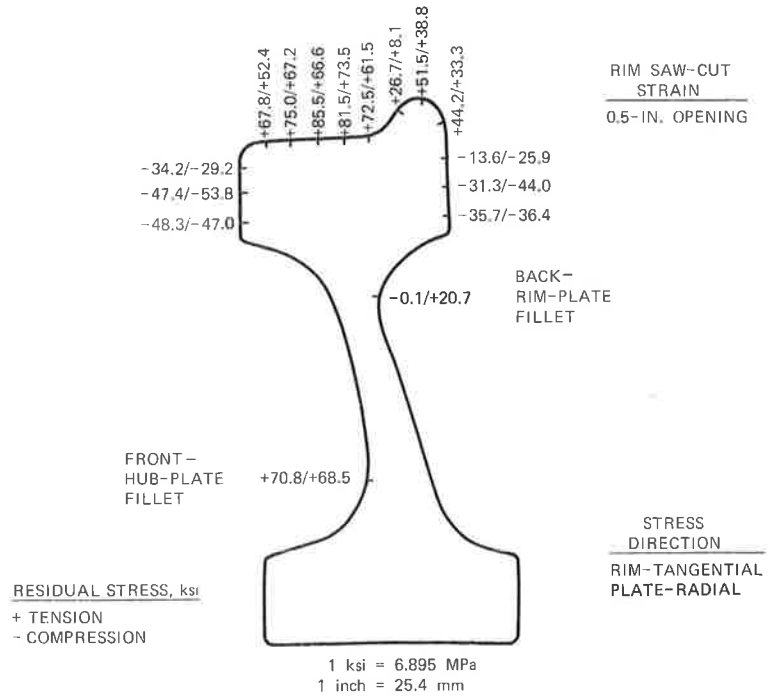

FIGURE 27. INDICATED RESIDUAL STRESSES IN NEW WHEEL NO. 1 (1-72-S-2476-A)

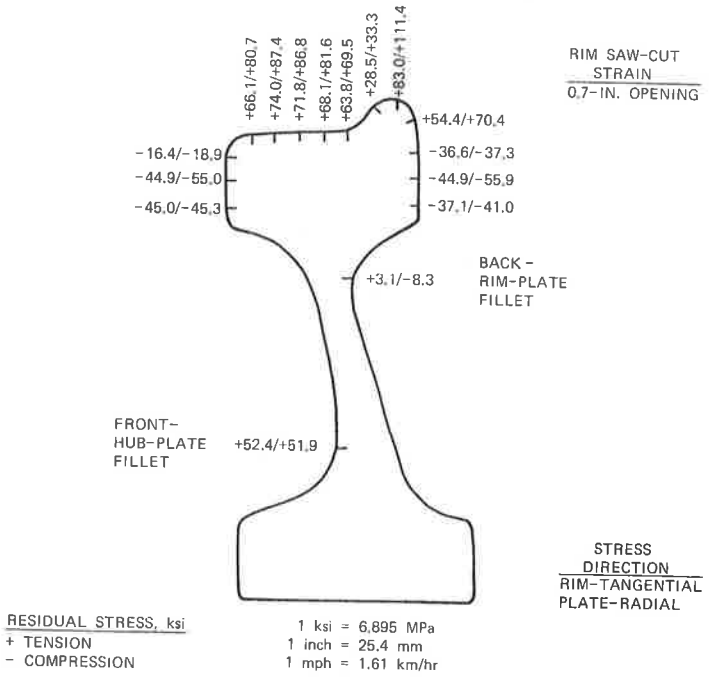

FIGURE 28. INDICATED RESIDUAL STRESSES IN NEW SHEEL NO. 2 (1-72-S-2474-A) AFTER 2424 SPEED-CONTROL BRAKING FROM 100 TO 50 MPH

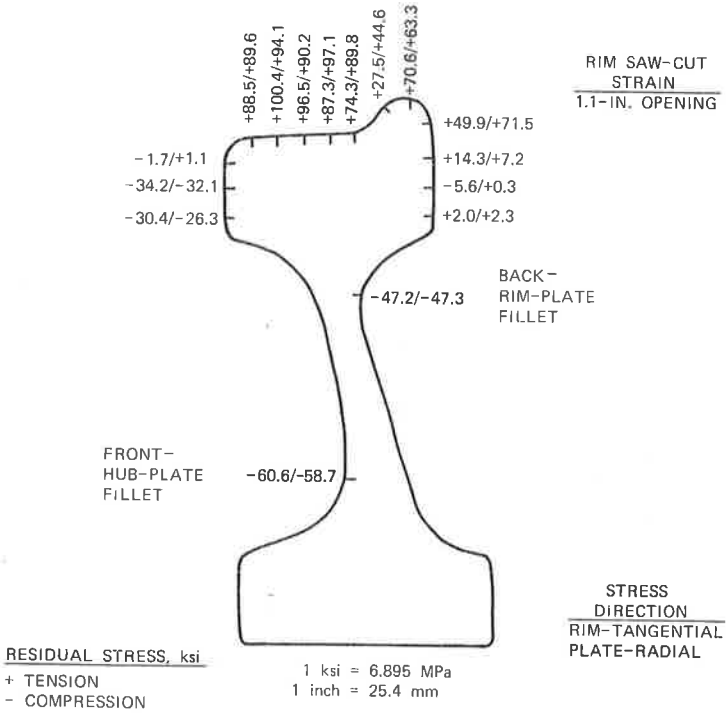

FIGURE 29. INDICATED RESIDUAL STRESSES IN NEW WHEEL NO. 3 (1-72-S-2472-A) AFTER COMBINATION OF DRAG BRAKING EMERGENCY-STOP BRAKING AND EMERGENCY-STOP BRAKING WITH WORNOUT BRAKESHOE

3.2.1 New, Untested Wheel

As part of the manufacturing process, rim-treated* railroad wheels are subjected to a heat treatment that increases the hardness of the rim for improved wear resistance. As a result, overall residual hoop compressive stresses are produced in the rim, and residual radial tensile stresses are produced in the critical plate fillets. The results of residual-stress studies of the new, untested wheel (No. 4) showed that the residual-stress pattern of this wheel was normal (see Figure 24), with compressive stresses in the outer 1-inch-thick (25.4 mm) layer of the rim. The rim saw-cut strain value of 1.3-inch (33 mm) closure also indicated that the overall residual hoop stress was compressive.

3.2.2 Used Wheels

During service, the as-manufactured wheel stresses are altered by the thermal effects of on-tread braking and by cold working of the tread surface by rolling loads. With regard to the residual-stress changes caused by braking, repeated severe of prolonged braking converts the rim stress from compression to tension and lowers (and sometimes reverses) the tensile stresses at the critical plate fillets. Conversely, rail contact loading induces compressive stresses into the tread surface. Because braking and rolling loads have opposite effects on the stresses in the tread areas, the independent magnitude of each effect cannot be readily determined. Nevertheless, the results of the residual-stress studies of the two used wheels showed that both wheels had been subjected to severe braking (see Figures 25 and 26). Evidence for this conclusion is the high residual tensile stress in the flange and the relatively low residual tensile stresses in the back-rim-plate fillets. (The back rim-plate fillet of wheel No. 6 was

*Essentially the same rim-treating practice is followed by all wheel manufacturers to increase the strength and hardness of the wheel rim. In this heat-treatment process, the wheel is heated to the austenitizing temperature, and only the rim portion is quenched. The rim and hub portions are then permitted to air-cool below the critical temperature before the wheel is tempered.

actually in compression.) The rim saw-cut strain values of 0.1- and 0.2-inch (2.5 and 5.1 mm) openings for wheels No. 5 and 6, respectively, indicate that both wheels had low overall residual hoop tensile stresses.

3.2.3 Dynamometer-Tested Wheels

The results of studies of the residual stresses in wheel No. 1, the wheel that had been subjected to 300 simulated emergency stops on the wheel-test machine, indicated that this wheel had developed high tensile stresses in the tread as well as in the flange (see Figure 27). These tensile stresses were much higher than those in the treads of the two used wheels because the wheel had not been subjected to rolling loads. The residual stresses in the critical plate fillets of this wheel were similar in magnitude to those in the used wheels. The rim saw-cut strain value for this wheel was 0.5-inch (12.7 mm) opening, indicating that the rim was in overall residual hoop tension.

The residual stresses in wheel No. 2, subjected to 2,424 speed-reduction braking on the wheel-test machine, were similar to those of wheel No. 1; high tensile stresses were present in the tread and flange, and the rim saw-cut strain velue was 0.7-inch (17.8 mm) opening, as shown in Figure 28.

Wheel No. 3 also had high residual hoop tensile stresses in the tread and flange (see Figure 29), but it had compressive stresses in the plate fillets. This wheel had been subjected to drag and emergency-stop braking with a wornout brakeshoe on the wheel-test machine. It is believed that the residual compressive stresses in the critical plate fillets were caused by the drag-braking cycles. In addition, the rim saw-cut strain value of 1.1-inch (27.9 mm) opening indicates that this wheel had the highest overall rim tensile stress of the wheels tested on the dynamometer. In wheel No. 3, the fine tread-surface cracks were initiated by the thermal alteration resulting from abnormal braking (that is, with wornout shoes). It is believed that stress concentrations at these cracks during subsequent brakings would cause the cracks to propagate by fatigue.

4. SUMMARY AND CONCLUSIONS

The wheels used on Metroliner cars reportedly develop thermal cracks during service even though the wheels are made from wheel-steel with a high resistance to thermal cracking. Therefore, the present study was conducted to determine the cause of the cracking.

One new wheel and two used wheels (one with a thermal crack developed in the tread during service) were examined for mechanical properties, macrostructure, microstructure, and residual stresses. Similar examinations were conducted on three new wheels which were first subjected to various braking cycles (on the laboratory dynamometer) designed to define the conditions that produce cracking.

The results of the study indicated that the wheel that had developed a thermal crack in service had been intermittently and severely heated around the tread surface and that such heating had altered the microstructure, produced residual tensile stresses, and permitted the crack to initiate. On the basis of this finding, it was hypothesized that the wheel had been braked with a wornout brakeshoe, a condition that could produce hot spots similar to those observed. This hypothesis was confirmed by results of studies of the dynamometer-tested wheels, which showed that emergency-stop braking with a simulated wornout brakeshoe could produce an altered microstructure and small thermal cracks similar in type to the crack in the service-cracked wheel. The results further indicated that neither altered microstructure nor cracking could be produced by numerous emergency or speed-reduction breakings with normal brakeshoes and forces.

APPENDIX A - U.S.S. RAILROAD WHEEL TESTING MACHINE

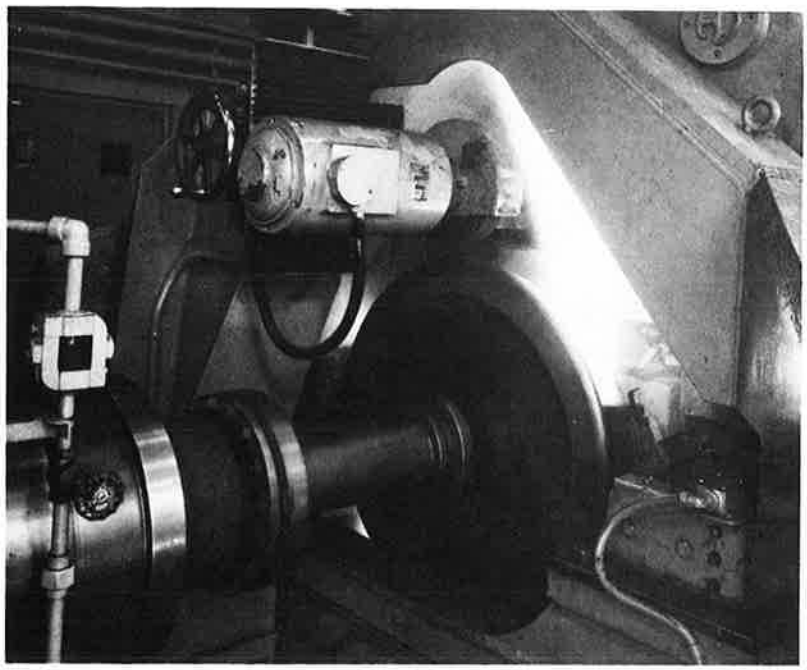

FIGURE A-1. SIMULATED EMERGENCY STOP OF PASSENGER CAR WHEEL FROM INITIAL SPEED OF 120 MPH SHOWS FLAMING OF BRAKESHOES

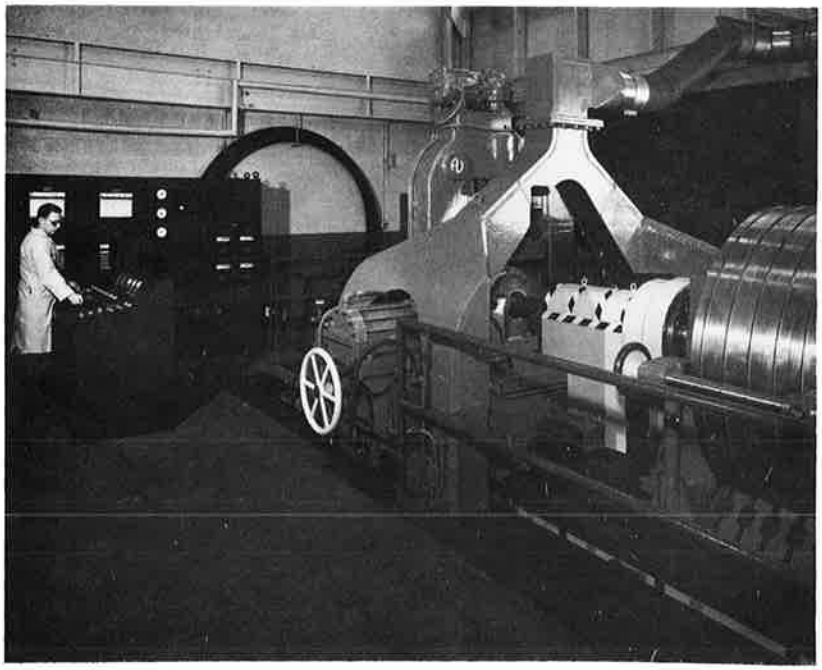

FIGURE A-2. GENERAL VIEW OF WHEEL TESTING MACHINE

APPENDIX B

DATA OBTAINED DURING STOP TEST OF NEW WHEEL NO. 1 (1-72-S-2476A)

Stop No.	Braking Time, sec	Braking Distance, ft	Total Work, 10^6 ft-lb	Stop No.	Braking Time, sec	Braking Distance, ft	Total Work, 10^6 ft-lb
1*	90	9125	NR	41	87	8630	11.2
2**	25	NR	NR	42	87	8560	11.2
3	96	8922	NR	43	87	8504	11.0
4	93	8851	11.9	44	87	8598	11.2
5	91	8824	NR	45	88	8813	11.6
6	91	8735	NR	46	89	8868	12.4
7	89	8600	13.3	47	91	8854	12.5
8	90	8654	12.3	48	91	8921	12.8
9	94	8257	NR	49	91	8774	12.8
10	93	8526	10.6	50	95	9501	13.4
11*	112	10756	11.7	51*	132	13135	12.1
12	97	9551	11.9	52	113	11341	11.6
13	95	9269	NR	53	107	10840	11.9
14	93	8980	NR	54	99	10065	11.7
15	93	9188	NR	55	98	9949	11.6
16**	24	3910	NR	56	97	9787	11.6
17	85	8159	11.5	57	93	9292	NR
18	87	8427	10.1	58	88	8930	NR
19	88	8575	10.6	59	87	8660	NR
20	90	8665	9.8	60	89	8727	NR
21	91	8997	NR	61	86	8230	13.2
22	86	8945	11.6	62	85	8183	NR
23	83	8331	9.8	63	83	8120	12.2
24	87	8701	9.8	64	83	8276	11.6
25	86	8519	NR	65	86	8353	13.1
26	87	8717	11.3	66	85	8212	11.5
27	85	8549	9.2	67	84	8103	13.2
28	84	8560	9.8	68	84	8291	12.5
29	86	8396	10.8	69	86	8498	13.3
30	87	8234	11.4	70	86	8342	12.9
31	88	8485	11.3	71	85	8424	12.5
32	89	8615	11.6	72	86	8325	12.4
33	87	8671	11.5	73	87	8384	11.1
34	89	8813	11.6	74	85	8238	13.3
35	87	8614	11.3	75	82	7970	13.5
36	87	8722	11.7	76	80	7668	13.5
37	88	8654	12.0	77	82	8049	13.4
38	88	8803	11.3	78	80	7867	13.6
39	88	8738	11.2	79	80	7829	11.9
40	87	8666	11.3	80	89	9539	13.0

Stop No.	Braking Time, sec	Braking Distance, ft	Total Work, 10^6 ft-lb	Stop No.	Braking Time, sec	Braking Distance, ft	Total Work, 10^6 ft-lb
81	87	8593	12.9	121	82	7949	12.8
82	84	8140	12.9	122	81	7951	12.8
83	84	8032	12.7	123	82	7856	13.1
84	86	8200	12.5	124	82	7893	11.5
85	87	8654	13.0	125	80	7712	11.3
86	85	8436	12.7	126	78	7568	12.8
87	87	8462	13.0	127	78	7613	11.5
88	86	8314	13.0	128	77	7375	11.4
89	84	7994	13.2	129	79	7590	10.9
90	83	8156	12.7	130	79	7684	12.6
91	82	8070	12.9	131	84	8264	13.1
92	88	8501	12.6	132	81	7962	12.8
93	89	8701	12.7	133	81	7959	12.9
94	87	8392	12.5	134	82	7842	13.1
95	88	8618	12.9	135	79	7639	12.5
96	89	8756	13.3	136	79	7671	12.9
97	86	8674	12.4	137	79	7634	12.8
98	89	8809	13.1	138	77	7439	12.9
99	90	8890	11.3	139	79	7909	12.7
100	86	8335	12.6	140	80	7824	12.8
101	88	8771	13.6	141	81	7804	12.6
102	86	8431	11.4	142	79	7578	12.7
103	87	8514	13.1	143	79	7718	12.7
104	91	8872	13.0	144	80	7738	12.8
105	89	8642	NR	145	78	7576	12.9
106	86	8330	13.1	146	83	8351	12.2
107	86	8387	12.4	147	83	8182	12.5
108	88	8476	12.9	148	83	8145	13.1
109	89	8716	13.2	149	82	7997	12.5
110	87	8525	13.1	150	82	8011	12.4
111*	138	14091	12.7	151	83	8108	13.7
112	121	12124	13.3	152	85	8480	13.5
113	109	10926	13.6	153	84	8293	12.8
114	99	9966	13.0	154	84	8297	13.1
115	94	9427	13.0	155	83	8057	12.0
116	92	9242	13.1	156	81	7963	12.5
117	90	8918	13.1	157	81	7846	12.7
118	89	8937	12.5	158	82	7962	12.8
119	87	8698	12.9	159	84	8196	13.0
120	84	8206	11.6	160	85	8404	12.4

Stop No.	Braking Time, sec	Braking Distance, ft	Total Work, 10^6 ft-lb	Stop No.	Braking Time, sec	Braking Distance, ft	Total Work, 10^6 ft-lb
161	89	8501	13.2	201	81	8078	12.8
162	87	8452	13.1	202	82	8029	13.0
163	85	8326	11.7	203	81	7932	12.8
164	85	8245	12.5	204	82	8043	13.4
165	84	8075	12.2	205	80	7937	13.3
166	80	7799	12.9	206	81	8044	13.7
167	83	8172	12.0	207	80	7942	13.8
168	83	8154	11.9	208	80	7885	13.2
169	84	8198	12.0	209	79	7759	13.5
170	83	8079	12.1	210	79	7807	13.0
171	86	8395	12.5	211	79	7799	NR
172	88	8534	11.6	212	85	8509	13.0
173	89	8682	12.0	213	81	8027	13.1
174	84	8026	12.0	214	83	8025	12.5
175	84	8205	12.5	215	78	7622	12.2
176	84	8213	13.1	216	78	7725	12.4
177	85	8331	11.4	217	78	7685	13.2
178	85	8398	11.4	218	82	8028	13.1
179	84	8361	12.2	219	79	7748	12.2
180	87	8677	12.6	220	82	7951	12.7
181	89	8710	12.4	221	78	7737	11.5
182*	128	13058	12.2	222	80	8006	11.5
183	116	11600	12.8	223	81	8025	13.2
184	113	11333	NR	224	82	8007	12.7
185	103	10351	13.0	225	82	8053	12.2
186	100	10028	12.0	226	80	7911	13.3
187	97	9767	13.7	227	81	7883	13.5
188	94	9549	12.0	228	80	7791	13.2
189	91	9145	12.5	229	79	7664	13.4
190	91	9090	13.4	230	82	8071	12.4
191	90	9057	12.8	231	79	7883	12.9
192	90	9046	12.9	232	82	8052	13.0
193	87	8769	13.0	233	84	8194	13.2
194	86	8556	NR	234	82	8075	NR
195	83	8299	13.1	235	86	8521	12.2
196	81	8014	12.2	236	83	8249	13.3
197	83	8401	12.8	237	85	8306	13.2
198	81	8168	12.4	238	86	8650	12.6
199	79	7744	12.6	239	95	9412	12.9
200	81	7987	12.7	240	85	8513	12.5

Stop No.	Braking Time, sec	Braking Distance, ft	Total Work, 10^6 ft-lb	Stop No.	Braking Time, sec	Braking Distance, ft	Total Work, 10^6 ft-lb
241	87	8683	14.0	271	117	11833	12.4
242	84	8093	13.2	272	103	10476	12.5
243	85	8304	13.6	273	100	10156	12.1
244	85	8469	12.9	274	98	9974	NR
245	91	8957	12.6	275	99	10155	12.5
246	87	8569	12.1	276	96	9825	12.6
247	85	8446	13.0	277	91	9218	12.8
248	84	8106	12.8	278	89	8909	12.9
249	87	8716	13.0	279	86	8488	13.0
250	87	8610	13.0	280	83	8206	12.7
251	85	8393	13.4	281	88	9069	12.5
252	86	8449	11.7	282	85	8470	12.2
253	86	8538	11.5	283	83	8248	12.2
254	94	9397	13.8	284	83	8052	11.9
255	88	8641	13.7	285***	210	12414	12.6
256	89	8775	12.4	286	84	8430	12.8
257	86	8412	12.2	287	82	8055	12.6
258	90	8840	13.0	288	81	7904	12.7
259	89	8290	13.3	289	81	7959	12.8
260	101	9340	13.0	290	80	7958	12.6
261	89	8644	12.7	291	80	7872	12.6
262	88	8661	12.9	292	83	8353	13.0
263	83	8228	13.3	293	82	8057	12.8
264	85	9247	13.1	294	81	7924	13.0
265	87	8799	13.4	295	79	7624	12.4
266	89	8872	12.0	296	79	7676	12.2
267	89	8756	12.1	297	80	7791	12.2
268	91	9044	12.2	298	78	7666	12.2
269	87	8679	12.4	299	78	7679	12.5
270*	131	13474	11.9	300	78	7765	13.4

* New brake shoe installed.
** Incomplete stop.
*** Low brake pressure.

NR = Not recorded.

Conversion Factors

1 ft = 0.3 m
1 ft-lb = 1.36 J

APPENDIX C

DATA OBTAINED DURING SPEED-REDUCTION BRAKED TEST OF NEW WHEEL NO. 2 (1-72-2474A)

Cycle No.	Braking Time, sec			Revolutions			Cycle No.	Braking Time, sec			Revolutions		
	1	2	3	1	2	3		1	2	3	1	2	3
1	Not Recorded			Not Recorded			36	32	33	34	376	396	404
2	33	34	35	381	394	408	37	31	32	34	361	379	405
3	33	35	35	375	397	400	38	30	32	33	362	385	397
4	32	33	34	405	381	396	39	29	31	33	337	355	386
5	33	34	33	380	398	390	40	31	34	35	368	395	402
6	32	34	34	352	392	396	41	31	32	33	353	385	391
7	34	34	34	376	403	402	42	30	32	34	355	380	393
8	31	33	35	356	371	398	43	30	32	34	355	383	401
9	32	34	35	373	396	409	44	29	32	34	336	383	410
10	32	33	34	378	387	394	45	29	31	33	363	373	396
11	32	33	35	375	387	401	46	31	33	33	372	388	393
12	32	33	35	370	385	402	46	30	33	33	358	389	390
13	31	34	34	360	395	415	48	32	32	33	369	369	390
14	NR	32	33	NR	382	392	49	29	31	33	333	365	394
15	32	34	35	384	398	403	50	30	34	35	354	394	411
16	30	33	34	358	392	407	51	30	32	34	355	372	393
17	32	32	35	375	378	406	52	30	34	34	356	392	394
18	34	35	31	399	420	367	53	30	32	33	355	377	386
19	31	32	32	351	383	389	54	31	32	34	355	371	400
20	30	32	33	345	369	393	55	30	31	32	344	367	382
21	32	32	33	372	381	394	56	30	31	34	350	370	400
22	31	33	34	375	391	403	57	32	32	35	381	381	404
23	31	33	34	359	389	406	58	29	31	33	344	370	399
24	31	32	34	362	373	404	59	32	30	34	376	356	396
25	32	33	35	379	400	407	60	28	30	32	324	347	381
26	31	32	34	365	383	410	61	28	31	32	325	382	391
27	32	33	34	378	399	408	62	33	34	35	379	403	414
28	32	33	35	372	390	411	63	31	32	33	366	372	390
29	31	33	34	364	389	409	64	28	29	30	330	340	354
30	31	33	33	370	386	396	65	28	31	31	334	357	364
31	33	33	33	390	391	391	66	28	31	33	324	374	398
32	31	39	34	365	444	408	67	29	31	33	334	361	389
33	34	36	39	404	435	479	68	30	31	32	342	368	379
34	31	33	32	363	385	370	69	29	31	32	343	367	376
35	32	33	32	373	396	386	70	28	31	34	325	361	391

Cycle No.	Braking Time, sec			Revolutions			Cycle No.	Braking Time, sec			Revolutions		
	1	2	3	1	2	3		1	2	3	1	2	3
71	29	32	32	339	370	373	106	31	33	34	375	393	411
72	29	30	33	341	350	385	107	31	33	34	371	396	400
73	NR	32	32	NR	365	378	108	32	33	33	364	397	410
74	29	29	32	341	352	376	109	31	32	34	362	384	408
75	28	30	33	323	348	381	110	31	32	36	362	386	423
76	46	48	52	549	580	601	111	30	32	34	354	376	403
77	31	33	35	413	404	415	112	30	33	33	353	384	388
78	34	34	35	401	403	414	113	29	32	35	348	380	410
79	34	34	35	390	396	405	114	33	34	34	386	401	406
80	33	33	34	390	390	400	115	31	33	34	368	394	404
81	33	33	33	383	393	394	116	31	33	34	364	388	403
82	31	32	33	368	379	394	117	31	33	36	365	388	422
83	32	32	33	386	387	394	118	33	33	35	382	391	407
84	29	31	32	340	365	373	119	31	33	34	374	388	406
85	28	31	32	330	356	368	120	31	33	33	362	395	391
86	28	31	34	332	378	397	121	31	34	33	367	401	389
87	32	35	35	379	405	405	122	32	32	33	381	389	405
88	33	35	35	388	407	415	123	30	31	33	344	372	403
89	32	33	34	383	399	397	124	32	33	34	376	394	404
90	32	34	34	379	409	403	125	29	32	33	342	376	386
91	31	34	34	376	403	408	126	30	31	33	349	369	372
92	33	34	34	389	409	408	127	30	33	33	354	380	384
93	32	34	35	384	406	418	128	29	31	32	339	363	373
94	31	33	33	371	397	414	129	29	31	32	343	370	374
95	32	34	35	381	396	419	130	30	31	31	352	361	364
96	34	35	35	397	415	410	131	30	32	33	355	370	392
97	32	34	34	381	401	399	132	31	31	33	360	366	387
98	32	34	34	378	406	417	133	35	32	33	403	369	386
99	31	33	36	365	385	429	134	30	32	34	359	380	403
100	33	34	35	390	401	407	135	32	33	36	376	392	420
101	32	34	35	380	391	406	136	31	33	34	370	383	396
102	33	34	34	387	400	407	137	30	30	31	350	363	375
103	32	33	36	380	392	430	138	29	31	32	337	360	370
104	31	33	31	364	402	381	139	29	30	33	343	356	387
105	33	34	34	383	411	411	140	31	31	34	363	370	416

Cycle No.	Braking Time, sec			Revolutions			Cycle No.	Braking Time, sec			Revolutions		
	1	2	3	1	2	3		1	2	3	1	2	3
141	31	32	34	358	380	407	176	39	NR	32	485	NR	385
142	32	32	34	372	378	397	177	30	31	33	349	368	392
143	30	31	32	348	360	372	178	30	31	34	347	360	393
144	28	29	32	330	343	374	179	28	30	33	350	352	382
145	30	31	33	345	369	392	180	30	30	32	349	355	383
146	30	32	31	352	375	370	181	30	30	32	349	355	373
147	29	30	32	344	359	377	182	28	30	31	339	356	371
148	28	30	31	332	355	366	183	36	30	31	451	342	351
149	28	30	31	334	357	358	184	28	30	31	332	354	367
150	29	31	33	338	365	381	185	31	NR	31	358	NR	366
151	62	61	56	703	690	632	186	30	30	30	368	364	343
152	31	33	33	365	384	387	187	27	29	NR	325	348	NR
153	31	31	32	372	377	379	188	29	31	31	333	369	374
154	31	32	32	362	384	382	189	28	30	30	327	348	358
155	31	32	32	367	380	377	190	28	28	31	326	325	355
156	32	32	34	372	381	406	191	27	30	32	314	346	379
157	30	32	35	346	384	404	192	29	31	32	342	365	374
158	32	33	33	379	387	391	193	30	30	31	346	354	368
159	32	32	33	376	374	389	194	28	30	31	328	345	362
160	30	33	33	355	391	390	195	29	29	31	341	349	360
161	31	32	38	337	362	443	196	28	31	33	329	361	380
162	34	36	36	380	417	420	197	27	29	31	306	336	355
163	33	33	34	383	395	398	198	27	31	32	328	362	373
164	33	33	33	384	385	387	199	29	30	32	335	354	366
165	32	33	32	374	386	379	200	28	31	32	394	363	373
166	32	33	33	374	384	384	201	28	30	32	334	349	370
167	33	NR	NR	373	NR	NR	202	27	29	32	318	342	378
168	30	30	32	360	364	382	203	28	30	32	328	355	371
169	36	31	32	445	363	374	204	29	31	33	338	364	387
170	31	32	34	356	382	403	205	29	31	33	337	364	388
171	31	32	34	364	379	398	206	28	30	32	336	349	371
172	31	33	33	370	384	397	207	30	33	33	351	358	371
173	31	31	33	364	361	387	208	30	30	32	350	362	382
174	30	34	32	353	383	374	209	29	31	32	324	340	362
175	30	31	32	357	367	385	210	28	29	31	316	347	356

Cycle No.	Braking Time, sec			Revolutions			Cycle No.	Braking Time, sec			Revolutions		
	1	2	3	1	2	3		1	2	3	1	2	3
211	27	30	30	316	357	356	246	26	30	30	310	342	350
212	28	30	31	324	351	372	247	28	28	30	329	328	355
213	27	28	31	323	330	369	248	26	29	30	304	339	360
214	28	30	31	336	347	361	249	27	29	32	311	332	365
215	28	29	29	328	337	349	250	37	41	41	486	490	485
216	27	28	31	316	336	359	251	31	33	34	362	383	393
217	27	30	30	376	349	359	252	30	31	31	352	356	368
218	28	29	30	321	346	350	253	27	30	33	335	349	381
219	27	31	32	313	362	383	254	28	29	31	332	344	363
220	27	30	32	318	345	375	255	28	29	31	329	338	359
221	30	32	33	351	374	385	256	28	29	31	332	344	363
222	29	31	31	347	358	368	257	28	29	31	329	358	379
223	28	30	32	328	357	377	258	30	31	31	431	361	366
224	27	30	33	317	354	388	259	30	31	32	349	355	376
225	29	30	32	336	353	369	260	29	30	32	339	355	381
226	28	30	32	329	358	374	261	30	30	30	358	351	350
227	28	29	32	330	347	373	262	29	29	32	338	341	371
228	27	31	33	321	363	389	263	30	29	NR	360	338	NR
229	27	29	31	317	336	358	264	31	32	34	370	374	397
230	28	30	32	332	356	371	265	30	31	32	354	329	374
231	28	31	33	329	371	398	266	30	27	31	359	376	383
232	28	28	32	324	333	384	267	30	32	33	356	375	384
233	27	30	31	326	357	380	268	31	32	32	358	355	379
234	29	30	32	341	361	382	269	31	31	32	358	367	378
235	29	30	31	341	353	370	270	29	31	32	347	363	373
236	26	29	29	304	337	345	271	29	30	31	336	356	368
237	29	30	32	337	347	378	272	28	30	32	334	355	382
238	38	26	30	472	311	352	273	27	30	31	324	354	369
239	30	31	31	350	364	371	274	28	30	32	330	349	381
240	28	29	28	317	334	330	275	28	29	31	324	335	353
241	26	29	30	313	344	353	276	28	30	32	338	349	372
242	NR	28	29	NR	325	338	277	28	30	31	328	353	366
243	25	29	30	296	339	352	278	28	30	31	329	351	363
244	NR	29	30	NR	339	397	279	29	30	32	339	359	377
245	25	28	29	297	330	322	280	29	30	31	347	358	371

Cycle No.	Braking Time, sec			Revolutions			Cycle No.	Braking Time, sec			Revolutions		
	1	2	3	1	2	3		1	2	3	1	2	3
281	31	34	37	376	396	413	316	28	30	31	326	353	362
282	27	29	30	320	343	356	317	28	29	30	329	347	362
283	26	29	29	304	331	336	318	27	28	29	314	331	348
284	28	30	32	323	356	370	319	26	28	30	309	326	350
285	28	29	31	324	337	374	320	NR	33	31	NR	381	363
286	26	29	33	304	333	379	321	27	29	29	312	332	341
287	26	29	33	304	333	379	322	26	27	29	301	303	337
288	29	30	33	342	351	380	323	26	29	29	299	334	334
289	28	30	32	321	352	375	324	28	29	29	324	337	339
290	NR	26	28	NR	302	320	325	27	28	29	310	328	333
291	25	26	27	300	301	317	326	42	43	43	492	493	492
292	25	27	28	297	321	356	327	34	35	36	396	404	423
293	27	27	29	312	314	343	328	32	34	34	370	392	402
294	26	27	29	306	320	344	329	30	32	33	347	367	381
295	26	28	29	308	330	341	330	31	31	33	364	367	385
296	28	29	32	330	348	382	331	30	31	32	358	364	379
297	29	30	32	330	348	376	332	NR	33	31	NR	382	370
298	28	30	32	332	347	365	333	30	31	33	356	371	383
299	26	28	30	311	331	353	334	30	31	31	349	357	366
300	29	33	32	337	388	368	335	31	31	31	361	360	366
301	27	28	29	312	328	340	336	32	30	33	374	352	384
302	27	29	30	311	335	346	337	30	31	31	354	359	367
303	27	29	30	321	341	355	338	30	31	32	350	363	378
304	26	29	29	306	339	346	339	31	31	33	366	360	384
305	27	29	30	320	334	341	340	31	31	31	360	364	361
306	27	29	30	325	343	349	341	32	30	32	351	320	363
307	27	29	30	316	334	351	342	31	30	31	357	346	354
308	28	29	30	324	341	351	343	28	30	32	330	353	369
309	28	29	31	327	334	359	344	30	30	31	351	353	361
310	28	30	31	323	348	364	345	30	30	32	345	352	372
311	28	29	32	324	339	369	346	30	31	31	349	370	368
312	27	29	27	313	346	329	347	30	30	32	345	350	366
313	28	29	32	327	347	374	348	31	31	33	364	366	383
314	28	29	33	330	344	387	349	32	30	33	367	346	377
315	28	30	32	333	359	381	350	29	29	30	339	325	342

Cycle No.	Braking Time, sec			Revolutions			Cycle No.	Braking Time, sec			Revolutions		
	1	2	3	1	2	3		1	2	3	1	2	3
351	33	33	32	386	378	374	386	27	28	29	312	327	337
352	31	31	32	357	360	369	387	27	28	29	313	324	334
353	31	31	31	362	352	362	388	28	29	32	323	334	361
354	29	31	32	342	366	371	389	NR	29	31	NR	334	355
355	32	30	33	377	346	381	390	27	29	30	325	346	357
356	30	30	31	344	350	364	391	49	49	51	576	575	591
357	30	30	30	345	344	350	392	34	36	35	397	422	420
358	32	28	33	363	308	292	393	37	37	38	364	360	370
359	28	30	31	325	356	362	394	28	28	28	329	329	328
360	28	30	31	328	351	364	395	31	27	30	355	324	352
361	30	31	32	346	361	377	396	27	29	32	307	341	367
362	30	30	31	344	350	363	397	28	30	31	331	347	365
363	30	30	31	351	349	365	398	32	30	31	373	353	365
364	31	30	31	365	352	367	399	30	29	31	350	343	359
365	29	30	30	335	349	352	400	30	30	31	356	360	371
366	29	30	31	336	350	367	401	30	31	30	356	366	355
367	30	30	31	340	344	365	402	28	29	32	328	337	377
368	28	29	30	326	341	347	403	29	30	31	334	356	365
369	28	29	30	323	339	351	404	29	31	32	341	356	376
370	30	29	30	347	338	354	405	30	31	33	347	358	388
371	29	29	31	331	338	353	406	29	29	33	337	342	383
372	30	29	32	347	339	380	407	31	31	31	360	367	363
373	28	29	30	322	341	353	408	27	29	31	315	339	362
374	29	31	30	341	354	347	409	27	28	32	311	333	384
375	31	29	31	353	339	355	410	27	29	29	311	334	345
376	27	29	30	314	334	346	411	26	28	29	307	335	336
377	31	29	32	362	340	370	412	28	28	31	322	325	360
378	27	29	29	317	337	337	413	25	27	31	301	317	357
379	27	29	29	320	338	340	414	31	29	32	355	343	374
380	29	29	31	336	334	356	415	28	32	33	333	367	387
381	27	29	30	314	335	342	416	29	28	31	335	328	358
382	30	29	30	349	337	342	417	29	31	32	341	366	371
383	29	29	30	343	334	344	418	29	31	32	338	361	371
384	27	29	30	315	334	346	419	27	29	32	317	334	370
385	29	28	30	331	359	355	420	28	31	32	325	361	384

Cycle No.	Braking Time, sec			Revolutions			Cycle No.	Braking Time, sec			Revolutions		
	1	2	3	1	2	3		1	2	3	1	2	3
421	28	30	31	322	356	363	456	27	29	29	310	336	340
422	29	32	34	339	378	394	457	26	28	29	298	325	339
423	28	30	32	340	358	379	458	27	29	30	314	331	349
424	28	30	30	334	352	358	459	26	28	31	306	325	356
425	27	30	30	319	350	346	460	28	28	29	329	324	332
426	26	29	30	311	340	364	461	26	28	29	299	320	338
427	27	29	30	316	332	349	462	27	28	29	316	323	337
428	28	30	30	322	345	360	463	26	27	29	301	317	332
429	28	29	32	323	351	373	464	26	28	30	308	331	355
430	27	29	30	311	335	350	465	28	29	30	319	330	348
431	27	31	32	319	355	371	466	27	29	29	310	335	344
432	27	28	28	319	332	332	467	27	29	29	307	337	336
433	28	30	31	318	345	360	468	27	28	31	312	324	361
434	28	31	31	326	357	365	469	27	29	30	311	338	352
435	28	29	31	322	339	358	470	27	28	29	309	322	339
436	28	31	32	328	358	361	471	27	28	29	311	317	332
437	27	30	31	317	348	365	472	25	26	27	300	302	315
438	28	30	32	330	355	379	473	27	27	27	318	311	311
439	28	30	32	328	354	369	474	26	26	27	302	298	312
440	29	31	33	343	370	383	475	37	42	41	432	483	477
441	28	30	32	327	347	373	476	34	35	35	393	406	409
442	27	31	35	310	362	408	477	33	33	33	379	384	383
443	29	31	33	339	373	382	478	30	32	33	353	370	384
444	29	32	31	340	369	362	479	31	33	33	362	386	384
445	29	30	31	337	355	361	480	31	31	33	368	364	380
446	40	29	30	488	334	352	481	32	31	33	375	362	386
447	27	29	30	309	336	351	482	30	32	33	354	375	383
448	26	29	30	320	347	362	483	30	31	33	360	367	384
449	27	31	31	319	352	362	484	31	32	34	368	371	398
450	28	29	30	323	345	353	485	31	31	32	361	369	380
451	27	29	31	318	338	362	486	31	32	33	367	375	397
452	27	27	28	313	315	325	487	31	32	33	362	375	385
453	27	28	30	317	327	349	488	31	32	33	373	383	393
454	27	28	29	313	327	340	489	33	31	33	385	370	389
455	27	28	29	317	328	336	490	31	31	33	366	357	377

Cycle No.	Braking Time, sec			Revolutions			Cycle No.	Braking Time, sec			Revolutions		
	1	2	3	1	2	3		1	2	3	1	2	3
491	29	31	33	358	367	387	526	30	30	34	357	353	402
492	33	31	34	389	363	413	527	30	31	32	343	369	370
493	30	31	33	343	359	390	528	35	30	30	415	352	351
494	33	30	34	370	348	402	529	28	29	30	323	339	349
495	32	33	35	379	390	412	530	27	29	30	314	339	354
496	30	30	31	349	356	379	531	27	29	29	313	339	341
497	29	NR	31	338	NR	370	532	25	27	28	298	314	336
498	34	29	30	402	335	351	533	29	29	30	327	338	349
499	31	31	34	364	359	383	534	26	29	30	306	343	357
500	29	30	31	343	352	364	535	27	30	30	317	345	342
501	30	30	32	385	356	371	536	27	27	29	316	319	342
502	29	30	30	343	348	355	537	27	29	30	315	341	343
503	29	28	29	332	342	343	538	27	30	30	319	343	353
504	30	NR	33	359	NR	381	539	28	29	30	322	343	352
505	28	32	32	329	359	351	540	27	29	31	325	341	363
506	28	30	30	304	321	341	541	28	30	31	320	347	360
507	26	28	30	340	369	372	542	28	29	32	326	345	360
508	29	30	31	340	353	361	543	28	29	30	323	339	367
509	29	30	31	340	362	380	544	27	29	31	323	345	354
510	29	30	30	342	351	356	545	28	29	32	316	342	353
511	29	30	31	327	359	363	546	27	30	32	327	345	371
512	29	31	32	338	358	373	547	28	30	32	318	345	373
513	29	31	31	339	360	363	548	28	30	30	320	339	337
514	27	30	31	315	353	364	549	27	30	31	316	345	341
515	26	27	31	322	323	356	550	27	30	30	318	338	343
516	27	31	30	323	359	359	551	28	31	32	330	345	369
517	29	30	31	339	355	357	552	29	30	33	335	357	379
518	27	31	31	323	359	365	553	35	31	32	413	356	376
519	27	30	32	322	352	361	554	29	31	34	332	363	392
520	30	31	33	350	358	368	555	30	29	33	344	336	418
521	29	31	32	337	364	373	556	29	31	33	328	363	389
522	30	30	32	348	353	370	557	26	25	27	304	299	314
523	29	30	31	435	368	370	558	24	26	28	284	310	326
524	29	29	30	346	343	361	559	38	39	40	438	448	460
525	28	31	32	330	366	372	560	32	33	34	360	380	382

Cycle No.	Braking Time, sec			Revolutions			Cycle No.	Braking Time, sec			Revolutions		
	1	2	3	1	2	3		1	2	3	1	2	3
561	31	32	31	367	372	369	596	26	28	29	309	329	338
562	29	30	30	334	356	355	597	26	28	28	307	329	332
563	34	30	30	380	348	353	598	26	27	29	305	314	330
564	29	29	31	334	342	362	599	26	27	29	303	322	332
565	30	31	32	352	357	375	600	27	29	29	311	333	344
566	30	30	31	351	359	361	601	28	28	32	329	327	374
567	28	30	31	328	348	368	602	29	30	30	338	353	356
568	28	30	32	330	358	364	603	28	30	30	327	348	344
569	28	29	31	330	346	364	604	27	28	28	319	338	333
570	36	29	30	438	346	355	605	27	27	28	319	316	330
571	29	30	31	332	357	363	606	26	28	27	304	328	319
572	27	29	30	317	342	355	607	26	27	NR	307	319	NR
573	28	29	31	327	342	363	608	26	28	28	307	323	328
574	28	29	30	324	344	356	609	26	28	28	310	323	321
575	28	28	29	321	326	343	610	25	27	29	292	314	327
576	28	29	30	324	345	356	611	65	40	40	527	492	483
577	27	30	30	326	350	354	612	32	32	32	373	373	372
578	28	29	31	332	336	363	613	29	30	30	339	352	358
579	29	30	30	328	350	349	614	27	29	31	313	345	365
580	28	30	30	333	350	356	615	29	29	29	342	337	341
581	28	29	31	330	345	359	616	28	29	30	326	345	356
582	28	30	31	328	347	371	617	31	31	32	374	365	380
583	28	30	32	334	356	377	618	31	33	31	360	390	350
584	29	30	32	341	360	379	619	31	31	32	368	359	375
585	26	28	29	306	324	346	620	37	34	30	459	397	348
586	31	30	31	344	337	359	621	30	29	31	351	334	357
587	40	29	34	492	344	391	622	31	31	31	372	369	366
588	25	29	30	310	336	355	623	31	30	32	361	353	368
589	26	29	31	309	336	358	624	29	30	31	347	353	370
590	38	28	29	418	333	357	625	28	31	32	338	351	374
591	26	28	30	310	334	356	626	28	31	30	331	364	349
592	27	28	31	311	328	354	627	26	28	30	313	333	347
593	26	27	30	309	326	357	628	27	28	31	316	334	364
594	26	28	31	315	338	363	629	29	29	30	337	337	353
595	26	27	30	310	326	349	630	26	29	31	310	346	369

Cycle No.	Braking Time, sec			Revolutions			Cycle No.	Braking Time, sec			Revolutions		
	1	2	3	1	2	3		1	2	3	1	2	3
631	27	29	31	324	346	361	666	26	27	30	316	339	364
632	25	26	28	292	303	371	667	30	28	30	343	328	350
633	27	28	29	320	325	340	668	30	28	30	320	346	352
634	25	27	29	295	323	336	669	28	29	31	325	334	360
635	26	28	28	310	328	330	670	26	27	30	308	317	345
636	27	28	29	318	327	338	671	28	31	32	320	362	374
637	28	27	29	325	311	338	672	25	26	28	291	308	322
638	26	27	29	304	320	337	673	26	26	30	303	304	341
639	28	29	28	328	340	332	674	32	27	30	389	319	340
640	27	28	28	327	336	338	675	26	27	31	301	320	358
641	30	29	43	356	337	487	676	41	45	41	494	527	485
642	27	28	31	315	337	364	677	31	34	32	373	397	379
643	30	28	39	346	328	484	678	28	29	30	330	333	355
644	28	28	30	332	332	352	679	29	30	29	336	354	338
645	27	30	28	310	348	323	680	29	30	30	338	348	345
646	27	28	30	313	333	349	681	28	29	31	327	338	351
647	26	27	30	305	318	341	682	29	29	29	348	344	343
648	26	26	28	306	306	326	683	32	29	29	377	335	337
649	26	27	30	310	320	353	684	33	33	30	388	386	351
650	26	27	29	305	315	336	686	26	26	28	306	306	331
651	25	27	27	296	314	314	686	26	29	30	312	350	350
652	23	25	28	258	292	328	687	24	25	27	249	294	345
653	27	27	28	309	315	324	688	26	26	27	308	303	334
654	25	26	27	291	303	318	689	29	30	30	334	348	352
655	25	26	26	293	302	312	690	27	28	30	313	327	343
656	25	26	27	297	306	316	691	29	30	30	333	352	357
657	27	26	28	309	305	323	692	28	30	31	323	345	360
658	26	26	26	307	303	308	693	25	28	30	310	329	343
659	26	26	27	300	304	324	694	27	30	30	319	354	352
660	26	26	28	300	312	324	695	27	27	28	314	315	327
661	29	29	31	341	341	360	696	26	28	28	308	323	331
662	39	30	31	441	334	360	697	27	27	29	319	325	337
663	28	31	31	327	368	354	698	27	28	29	316	323	336
664	28	29	30	326	347	353	699	29	27	28	327	320	-
665	28	29	31	326	334	360	700	28	30	32	325	303	347

Cycle No.	Braking Time, sec			Revolutions			Cycle No.	Braking Time, sec			Revolutions		
	1	2	3	1	2	3		1	2	3	1	2	3
701	27	27	28	312	315	330	736	25	26	28	296	303	330
702	26	28	28	310	327	331	737	26	27	28	314	317	325
703	26	28	30	307	328	348	738	27	27	29	320	311	345
704	27	28	29	311	332	343	739	26	27	29	307	316	321
705	26	29	30	300	336	347	740	40	40	39	471	477	450
706	26	28	29	304	318	331	741	31	NR	35	358	NR	412
707	25	28	30	290	324	344	742	32	28	28	376	327	324
708	26	28	NR	309	330	NR	743	26	28	29	308	324	336
709	28	30	30	326	340	341	744	25	28	30	295	326	347
710	27	29	30	310	332	344	745	27	28	33	329	321	399
711	28	28	31	320	327	366	746	27	30	31	321	348	363
712	27	29	33	318	337	390	747	26	30	31	308	341	356
713	28	28	29	325	326	336	748	27	30	31	322	342	355
714	29	29	29	338	335	337	749	26	30	29	311	340	333
715	28	29	30	324	332	351	750	26	27	29	305	318	333
716	27	25	25	307	291	300	751	30	28	29	349	330	341
717	25	26	28	299	306	328	752	28	27	29	331	321	337
718	26	26	28	305	305	324	753	28	28	29	322	329	334
719	28	26	29	323	305	333	754	28	29	30	327	337	351
720	26	27	29	304	319	342	755	28	28	30	328	330	348
721	28	30	32	321	357	385	756	29	31	30	332	369	348
722	27	30	29	309	353	346	757	30	28	29	342	331	341
723	26	28	29	305	319	337	758	27	29	30	309	334	345
724	26	28	31	306	325	363	759	27	28	29	320	327	342
725	25	27	31	295	311	352	760	26	27	27	302	318	319
726	28	27	28	317	309	322	761	26	28	32	303	327	373
727	27	29	30	313	343	349	762	26	28	31	306	328	363
728	25	29	29	298	334	334	763	26	28	30	303	329	345
729	26	28	28	299	328	330	764	27	28	29	310	322	337
730	26	28	29	301	327	339	765	27	27	29	312	317	331
731	25	25	26	296	291	301	766	29	30	33	339	351	382
732	23	25	27	274	288	315	767	26	31	30	304	361	352
733	25	26	27	295	305	315	768	28	30	29	323	351	339
734	25	26	29	291	308	332	769	26	26	25	303	306	300
735	26	27	28	310	314	320	770	24	27	27	287	312	313

Cycle No.	Braking Time, sec			Revolutions			Cycle No.	Braking Time, sec			Revolutions		
	1	2	3	1	2	3		1	2	3	1	2	3
771	26	26	28	303	309	331	806	27	27	28	313	313	328
772	27	29	27	317	336	322	807	27	27	27	318	311	322
773	25	27	29	298	313	340	808	29	26	27	322	300	319
774	28	27	29	328	317	339							
775	25	28	28	298	327	351							
776	28	29	29	325	341	338							
777	27	29	29	321	344	352							
778	27	27	28	313	312	323							
779	26	28	28	308	326	328							
780	27	27	30	316	313	340							
781	27	29	31	325	337	363							
782	28	28	30	321	322	352							
783	38	29	28	478	329	330							
784	26	27	28	306	319	327							
785	26	28	28	307	323	331							
786	27	28	28	317	330	337							
787	26	28	28	302	328	330							
788	28	28	31	327	330	346							
789	25	24	26	291	271	299							
790	24	25	27	280	290	313							
791	35	36	38	405	420	443							
792	30	29	31	335	339	362							
793	27	28	29	311	337	337							
794	37	29	31	455	346	357							
795	26	28	29	322	328	343							
796	28	30	33	326	346	365							
797	27	28	31	325	344	365							
798	26	28	30	315	322	352							
799	27	30	31	317	342	352							
800	27	28	30	312	336	344							
801	26	28	30	311	328	342							
802	26	28	30	312	327	345							
803	26	28	29	310	328	344							
804	26	26	28	307	323	335							
805	26	25	26	303	290	298							

Note:

NR = not recorded.

APPENDIX D

STRAINS AND TEMPERATURE DEVELOPED DURING SPEED-REDUCTION BRAKING TESTS OF WHEEL NO. 2

Part of Cycle	Radial Strain,* μ in./in.		Temperature, °F	
	FHPF++	BRPF++	1/16-in. Depth	1/4-in. Depth
Cycle No. 1				
After first brake application**	640	480	440	270
" second " " **	1860	1080	500	350
" third " " ***	2830	1480	530	400
" fourth " " ****	4440	2220	600	500
" cooling	1880	90	80	80
Cycle No. 2				
After first brake application+	1070	840	400	+++
" second " " +	1750	1490	550	+++
" third " " +	2270	1900	590	450
" cooling	0	0	80	80
Cycle No. 13				
After first brake application+	1000	990	+++	+++
" second " " +	1750	1590	+++	+++
" third " " +	2260	1980	590	410
" cooling	0	0	80	80
Cycle No. 80				
After first brake application+	880	710	+++	+++
" second " " +	1590	1390	+++	+++
" third " " +	2080	1810	590	440
" cooling	0	0	80	80
Cycle No. 220				
After first brake application+	920	1030	+++	+++
" second " " +	1620	1650	+++	+++
" third " " +	2100	1910	+++	+++
" cooling	0	0	+++	+++
Cycle No. 352				
After first brake application+	1075	1735	+++	+++
" second " " +	1090	1650	+++	+++
" third " " +	2210	1955	+++	+++
" cooling	0	0	+++	+++

* The temperatures of the plate fillets did not exceed 250°F; no corrections were required.
** Brake only to 565 rpm.
*** Brake only to 535 rpm.
**** Brake only to 0 (complete stop).

\+ Brake to 465 rpm.
++ FHPF = Front-hub-plate fillet.
BRPF = Back-rim-plate fillet.
+++ Unreliable thermocouple because of moisture.
Note: Cycle No. 1 resulted in plastic deformation of the FHPF. Cycles No. 2 through 808 did not produce plastic deformation of the FHPF.

Conversion Factors

°C = 5/9(°F - 32)
1 inch = 25.4 mm

APPENDIX E

DATA OBTAINED DURING DRAG-BRAKING/EMERGENCY-STOP BRAKING TEST OF NEW WHEEL NO. 3 (1-72-S-2472A)

Cycle	Type of Braking	Stop Time, sec	Max Temp,* °F	Partial Radial Residual Stress at Back-Rim-Plate Fillet,** ksi	
				Gage No. 1	Gage No. 2
1***	Drag		960	-37	-26
2***	"		900	-90	-59
3***	Stop	90	680		
4	"	85	710		
5	"	85	720		
6	"	87	710		
7	"	86	730	-90	-44
8	"	88	720		
9	"	87	720		
10	"	83	630		
11	"	82	640		
12	"	84	700	-49	-15
13***	Drag		920	-99	-70
14***	"		920	-104	-67
15***	Stop	78	820		
16	"	70	700		
17	"	71	700		
18	"	72	750		
19***	"	87	600	-54	-30
20	"	72	780		
21	"	71	790		
22	"	75	700		
23	"	78	700		
24	"	76	750	-51	-22
25	"	78	-		
26	"	83	790		
27	"	81	800		
28	"	81	820		
29	"	83	790	-44	-31
30	"	77	750		
31	"	80	640		
32	"	82	720		
33	"	82	650		
34	"	81	650	-46	-19
35	"	85	610		
36	"	87	720		
37	"	86	600		
38	"	83	620		
39	"	84	740	-31	-4
40	"	91	700		
41	"	86	600		
42	"	86	650		
43	"	90	780		

Cycle	Type of Braking	Stop Time, sec	Max Temp,*°F	Partial Radial Residual Stress at Back-Rim-Plate Fillet,** ksi	
				Gage No. 1	Gage No. 2
44	Stop	83	650	-25	-2
45	"	86	680		
46	"	94	640		
47	"	88	640		
48	"	85	750		
49	"	83	670		
50	"	93	690		
51	"	91	870		
52	"	84	650		
53	"	91	700		
54	"	88	650	-20	0
55	"	80	600		
56	"	86	600		
57	"	90	660		
58	"	86	640		
59	"	84	620		
60****	"	125	690		
61	"	136	630		
62	"	132	720		
63	"	105	910		
64	"	105	680	-17	+8
65	"	95	880		
66	"	55	820		
67****	"	102	580		
68	"	94	820		
69	"	130	600		
70***	"	84	530		
71	"	79	510		
72	"	79	530		
73	"	76	560		
74	"	75	600	-20	+14
75	"	75	600		
76	"	76	580		
77	"	75	600		
78	"	79	590		
79	"	78	680		
80	"	75	620		
81	"	75	600		
82	"	77	730		
83	"	77	600		
84	"	80	650		
85	"	79	600		
86	"	77	660		
87	"	77	800		
88	"	79	620		
89	"	76	600		

Cycle	Type of Braking	Stop Time, sec	Max Temp,*°F	Partial Radial Residual Stress at Back-Rim-Plate Fillet,** ksi	
				Gage No. 1	Gage No. 2
90	Stop	78	640		
91***	"	79	800		
92	"	90	440		
93	"	85	520		
94	"	78	670		
95	"	120	620		
96	"	107	620		
97	"	103	610		
98	"	96	610		
99	"	92	600		
100	"	94	590		
101	"	89	590		
102	"	89	590		
103	"	97	620		
104	"	95	640		
105	"	84	610		
106	"	84	690		
107	"	84	610		
108	"	83	690		
109	"	76	670		
110	"	75	680		
111	"	75	830		
112	"	74	720		
113	"	76	700		
114	"	72	710	-26	-14

* 1/8 Inch (3.2 mm) beneath tread surface at center.
** Caused by dynamometer testing. Front-hub-plate-fillet gages were destroyed; no data were obtained.
*** New brake shoe installed.
**** Simulated wornout brakeshoe installed.

Conversion Factor

1 ksi = 6.895 MPa

APPENDIX F

RESIDUAL-STRESS DATA*

Strain Gage	Strain, μin./in. ε_o	ε_f	ε	Indicated Residual Stress,** ksi	Strain Gage	Strain, μin./in. ε_o	ε_f	ε	Indicated Residual Stress,** ksi
			Wheel No. 4 (1-72-S-2466A)						
Rim 1-1	8410	9440	-1030	-30.9	Rim 1-2	7550	8680	-1130	-33.9
2-1	7830	9050	-1220	-36.6	2-2	7785	9150	-1365	-41.0
3-1	8960	10360	-1400	-42.0	3-2	8295	9880	-1585	-47.5
4-1	8660	10130	-1470	-44.1	4-2	8945	10640	-1695	-50.9
5-1	6985	8450	-1465	-43.9	5-2	9025	10820	-1795	-53.9
6-1	7545	9130	-1585	-47.5	6-2	8675	10510	-1835	-55.0
7-1	8230	9960	-1730	-51.9	7-2	8440	10420	-1980	-59.4
8-1	9225	10760	-1535	-46.0	8-2	8747	10640	-1895	-56.9
9-1	8360	9680	-1320	-39.6	9-2	8470	9980	-1510	-45.3
10-1	8365	9820	-1455	-43.6	10-2	7180	8760	-1580	-47.4
11-1	8810	10500	-1690	-50.7	11-2	8710	10620	-1910	-57.3
12-1	8415	9440	-1025	-30.4	12-2	8825	10080	-1255	-37.6
13-1	9005	10340	-1335	-40.0	13-2	8825	10510	-1685	-50.5
14-1	8105	9870	-1765	-53.0	14-2	8300	10280	-1980	-59.4
FHPF-1-R	7935	4690	+3245	+110.1	FHPF-2-R	7650	4630	+3020	+109.1
D	9490	7400	+2090		D	8495	6480	+2015	
T	7995	7160	+835	+54.7 $\alpha = 90°$	T	7506	6640	+965	+61.7 $\alpha = 90°$
BRPF-1-R	7555	6460	+1095	+34.5	BRPF-2-R	7405	5530	+1875	+64.2
D	8970	8490	+480		D	9150	8280	+870	
T	7510	7640	-130	+6.5 $\alpha = 90°$	T	7725	7520	+205	+24.8 $\alpha = 83°$

Strain Gage	Strain, μin./in. ε_o	ε_f	ε	Indicated Residual Stress,** ksi	Strain Gage	Strain, μin./in. ε_o	ε_f	ε	Indicated Residual Stress,** ksi
			Wheel No. 6 (1-71-S-10190A)						
Rim 1-1	9685	10370	-685	-20.5	Rim 1-2	7950	8820	-870	-26.1
2-1	8990	10380	-1390	-41.7	2-2	9310	10840	-1530	-45.9
3-1	9060	9820	-760	-22.8	3-2	9240	9910	-670	-20.1
4-1	8030	7410	+620	+18.1	4-2	8565	8230	+335	+10.0
5-1	8840	8590	+250	+7.5	5-2	8380	8400	-20	-0.6
6-1	8735	8720	+15	+0.5	6-2	9010	8770	+240	+7.2
7-1	7325	7450	-125	-3.8	7-2	7740	7790	-50	-1.5
8-1	9170	9580	-410	-12.3	8-2	8555	8700	-345	-10.4
9-1	9490	8060	+1430	+42.9	9-2	8860	7800	+1060	+31.8
10-1	9655	7500	+2155	+64.6	10-2	9080	6780	+2300	+69.0
11-1	8905	7310	+1595	+47.9	11-2	8870	7280	+1590	+42.8
12-1	8800	9540	-740	-22.2	12-2	8900	9150	-250	-7.5
13-1	8635	9550	-915	-27.4	13-2	7775	8570	-795	-24.8
14-1	8905	9300	-395	-11.8	14-2	8910	9420	-510	-15.3
FHPF-1-R	7530	6130	+1400	+49.3	FHPF-2-R	7730	6610	+1120	+40.6
D	ND	ND	ND		D	8920	8160	+760	
T	7075	6760	+315	+24.2	T	7650	7280	+370	+23.2
				α = ND					α = 90°
BRPF-1-R	8270	8370	-100	-3.7	BRPF-2-R	8350	8960	-610	-22.5
D	9155	9200	-45		D	9415	9750	-335	
T	7450	7650	-200	-9.1	T	7675	7880	-205	-12.5
				α = 87°					α = 80°

Strain Gage	Strain, μin./in. ε_o	ε_f	ε	Indicated Residual Stress,** ksi	Strain Gage	Strain, μin./in. ε_o	ε_f	ε	Indicated Residual Stress,** ksi
			Wheel No. 1 (1-72-S-2476A)						
Rim 1-1	4925	6535	-1610	-48.3	Rim 1-2	5580	7145	-1565	-47.0
2-1	5480	7060	-1580	-47.4	2-2	4445	6240	-1795	-53.8
3-1	5350	6590	-1140	-34.2	3-2	5640	6615	-975	-29.2
4-1	5735	3475	+2260	+67.8	4-2	5575	3830	+1745	+52.4
5-1	5050	2550	+2500	+75.0***	5-2	5165	2920	+2245	+67.2
6-1	5455	2600	+2855	+85.5***	6-2	5360	3140	+2220	+66.6
7-1	5108	2390	+2720	+81.5***	7-2	4520	2070	+2450	+73.5***
8-1	4640	2220	+2420	+72.5***	8-2	5560	3510	+2050	+61.5
9-1	5525	4435	+890	+26.7	9-2	5700	5430	+270	+8.1
10-1	4580	2865	+1715	+51.5	10-2	5850	4555	+1295	+38.2
11-1	4455	2980	+1475	+44.2	11-2	5730	4620	+1110	+33.3
12-1	5980	7170	-1190	-35.7	12-2	6545	7760	-1215	-36.4
13-1	4305	5350	-1045	-31.3	13-2	5125	6590	-1465	-44.0
14-1	5490	5945	-455	-13.6	14-2	5820	6685	-865	-25.9
FHPF-1-R	4010	2025	+1985	+70.8	FHPF-2-R	3930	1980	+1950	+68.6
D	5595	1210	+1385		D	5230	4000	+1230	
T	3955	3350	+605	+40.2 $\alpha = 90°$	T	3960	3445	+515	+36.9 $\alpha = 90°$
BRPF-1-R	3770	3745	-25	-0.1	BRPF-2-R	3730	3080	+650	+20.7
D	6240	6835	-595		D	5885	5540	+345	
T	4270	4780	-510	-20.5 $\alpha = 108°$	T	3810	3870	-60	++4.1 $\alpha = 90°$

Strain Gage	Strain, μin./in. ε_o	ε_f	ε	Indicated Residual Stress,** ksi	Strain Gage	Strain, μin./in. ε_o	ε_f	ε	Indicated Residual Stress,** ksi
			Wheel No. 5 (1-71-S-10191A)						
Rim 1-1	8850	10230	-1380	-41.4	Rim 1-2	8655	10430	-1775	-53.5
2-1	8590	10390	-1800	-54.0	2-2	9090	11360	-2270	-68.0
3-1	9980	10390	-410	-12.3	3-2	9555	10520	-965	-28.9
4-1	9285	8890	+395	+11.8	4-2	8080	7790	+290	+8.7
5-1	8945	8660	+275	+8.2	5-2	9600	9290	+310	+9.3
6-1	8915	8570	+375	+11.2	6-2	8510	8260	+250	+7.5
7-1	7410	7350	+60	+1.8	7-2	8070	7920	+150	4.5
8-1	9025	9430	-425	-12.7	8-2	8600	8970	-370	-11.1
9-1	8800	7830	+970	+29.0	9-2	9030	7910	+1120	+33.6
10-1	8755	6380	+2375	+71.2***	10-2	8185	5990	+2195	+65.9
11-1	8800	7500	+1300	+39.0	11-2	8415	6540	+1875	+56.7
12-1	8630	9720	-1090	-32.7	12-2	8525	8890	-1365	-40.9
13-1	7920	9060	-1040	-31.2	13-2	9005	11220	-2195	-65.9
14-1	8935	10050	-1115	-33.4	14-2	8730	10270	-1540	-45.6
FHPF-1-R	8055	5920	+2135	+75.1***	FHPF-2-R	7770	5670	+2100	+73.1***
D	9285	7680	+1605		D	8465	7110	+1365	
T	8240	7930	+310	+39.5	T	7685	7130	+555	+40.5
				$\alpha = 81.5°$					$\alpha = 88°$
BRPF-1-R	7795	7560	+235	+9.5	BRPF-2-R	7750	7350	+400	+15.7
D	9310	9210	+100		D	9490	9120	+370	
T	7416	7310	+105	+5.1	T	8075	7840	+235	+11.3
				$\alpha = 113.5°$					$\alpha = 73.5°$

Strain Gage	Strain, μin./in. ε_o	ε_f	ε	Indicated Residual Stress,** ksi	Strain Gage	Strain, μin./in. ε_o	ε_f	ε	Indicated Residual Stress,** ksi
			Wheel No. 2 (1-72-S-2474A)						
Rim 1-1	7550	9050	-1500	-45.0	Rim 1-2	6540	8050	-1510	-45.3
2-1	6695	8190	-1495	-44.9	2-2	6970	8800	-1830	-55.0
3-1	6610	7155	-545	-16.4	3-2	6515	7145	-630	-18.9
4-1	6680	4475	+2200	+66.1	4-2	6295	3600	+2690	+80.7***
5-1	6750	4285	+2465	+74.0***	5-2	6515	3605	+2910	+87.4***
6-1	7320	4925	+2395	+71.8***	6-2	6390	3495	+2895	+86.8***
7-1	6890	4620	+2270	+68.1	7-2	6450	3730	+2720	+81.6***
8-1	7880	5755	+2125	+63.8	8-2	6185	3870	+2315	+69.5
9-1	6520	5570	+950	+28.5	9-2	6710	4595	+1110	+33.3
10-1	7070	4305	+2765	+83.0***	10-2	6955	3240	+3715	+111.4***
11-1	6675	4865	+1815	+54.4	11-2	6380	4030	+2350	+70.4
12-1	6770	8005	-1235	-37.1	12-2	8005	9370	-1365	-41.0
13-1	7495	8995	-1495	-44.9	13-2	6425	8290	-1865	-55.9
14-1	7490	8710	-1220	-36.6	14-2	7545	8785	-1245	-37.3
FHPF-1-R	8420	6960	+1460	+52.4	FHPF-2-R	7675	6276	+1400	+51.9
D	7520	6525	+995		D	6985	5945	+1040	
T	8210	7767	+445	+29.0	T	8370	7800	+570	+32.7
				α = 87.5°					α = 86.5°
BRPF-1-R	8680	8535	+145	+3.1	BRPF-2-R	7315	7480	-165	-8.3
D	7785	7975	-190		D	7695	8050	-355	
T	8550	8945	-395	-9.5	T	8030	8395	-365	-14.6
				α = 97°					α = 117°

Strain Gage	Strain, μin./in. ε_o	ε_f	ε	Indicated Residual Stress,** ksi	Strain Gage	Strain, μin./in. ε_o	ε_f	ε	Indicated Residual Stress,** ksi
			Wheel No. 3 (1-72-S-2472A)						
Rim 1-1	7736	8750	-1014	-30.4	Rim 1-2	6007	6883	-876	-26.3
2-1	6356	7495	-1139	-34.2	2-2	7546	8615	-1069	-32.1
3-1	7955	8013	-58	-1.7	3-2	7677	7640	+37	+1.1
4-1	7254	4305	+2949	+88.5***	4-2	8174	5187	+2987	+89.6***
5-1	6585	3240	+3345	+100.4***	5-2	6963	3825	+3138	+94.1***
6-1	6950	3734	+3216	+96.5***	6-2	5696	2688	+3008	+90.2***
7-1	6654	3745	+2909	+87.3***	7-2	7343	4105	+3238	+97.1***
8-1	7393	4915	+2478	+74.3***	8-2	7232	4240	+2992	+89.8***
9-1	6883	5965	+918	+27.5	9-2	7427	5942	+1485	+44.6
10-1	7413	5060	+2353	+70.6	10-2	6606	4496	+2110	+63.3
11-1	6630	4966	+1664	+49.9	11-2	7330	4946	+2384	+71.5***
12-1	6458	6393	+65	+2.0	12-2	6846	6768	+78	+2.3
13-1	6880	7066	-186	-5.6	13-2	6504	6495	+9	+0.3
14-1	6810	6332	+478	+14.3	14-2	6900	6660	+240	+7.2
FHPF-1-R	7774	9506	-1732	-60.6	FHPF-2-R	7345	8989	-1644	-58.7
D	7330	8320	-990		D	7583	8546	-963	
T	6825	7185	-360	-29.0 $\alpha = 89°$	T	7614	8054	-440	-30.7 $\alpha = 88°$
BRPF-1-R	6640	8063	-1423	-47.2	BRPF-2-R	7032	8445	-1413	-47.3
D	7287	8057	-770		D	7530	8270	-740	
T	7090	7116	-26	-15.0 $\alpha = 91°$	T	7415	7488	-73	-16.3 $\alpha = 90°$

NOTE: ε_o = strain value before cutting.
ε_f = strain value after cutting.
$\varepsilon = \varepsilon_o - \varepsilon_f$ = relaxation strain.

\+ indicates tension.
\- indicates compression.

FHPF = Front-hub-plate fillet.
BRPF = Back-rim-plate fillet.

* A Young's modulus of 30×10^6 psi and a Poisson's ratio of 0.3 were used for the calculations.
** Also listed is α, the angle between the normal strain and the maximum principal stress directions.
*** The yield point was possibly exceeded.

Conversion Factors

1 ksi = 6.895 MPa
1° = 0.017 rad
1 inch = 25.4 mm

APPENDIX G

SAW-CUT STRAIN DATA

Wheel No.	Rim Punch Mark	Distance Between Punch Marks, inches		
		Initial	After Saw Cuts	Change
1	Inner front	2.00	2.50	+0.50
	Outer front	2.00	2.56	+0.56
	Inner back	2.00	2.5	+0.50
	Outer back	2.00	2.56	+0.56
2	Inner front	2.00	2.71	+0.71
	Outer front	2.00	2.65	+0.65
	Inner back	2.00	2.71	+0.71
	Outer back	2.00	2.65	+0.65
3	Inner front	2.00	3.06	+1.06
	Outer front	2.00	3.12	+1.12
	Inner back	2.00	3.06	+1.06
	Outer back	2.00	3.12	+1.12
4	Inner front	2.00	0.71	-1.29
	Outer front	2.00	0.59	-1.41
	Inner back	2.00	0.71	-1.29
	Outer back	2.00	0.56	-1.44
5	Inner front	2.00	2.07	+0.07
	Outer front	2.00	2.08	+0.08
	Inner back	2.00	2.08	+0.08
	Outer back	2.00	2.09	+0.09
6	Inner front	2.00	2.24	+0.24
	Outer front	2.00	2.27	+0.27
	Inner back	2.00	2.25	+0.25
	Outer back	2.00	2.29	+0.29

\+ indicates opening (tension)
\- indicates closing (compression)

Conversion Factor

1 inch = 25.4 mm

APPENDIX H

REPORT OF INVENTIONS

No inventions or discoveries were made or conceived, or for the first time actually reduced to practice by U.S. Steel, its employees, its subcontractors, or their employees, in the course of, in connection with, or under the terms of this contract. However, this study contract does represent an improved understanding of the propagation of microstructure cracking to thermal cracking.

The results further indicated that neither altered microstructures nor cracking could be produced by many emergency brakings or speed-reduction brakings with normal brakeshoes and forces.

310 copies